Studies on the effects and mechanisms of dietary collagen hydrolysate and sphingomyelin on skin aging

Chisato Oba

2018

CONTENTS

GENERAL INTRODUCTION

Skin provides an effective barrier between the organism and the environment by helping to reduce the risk of physical, chemical, and microbial damage. The skin mainly consists of epidermis and dermis. The epidermis is an outmost layer of the skin, contains keratinocytes, melanocytes, immune cells. Epidermal keratinocytes are divided from the basement membrane and move upward toward the skin surface. Corneocytes are terminally differentiated keratinocytes. The stratum corneum (SC), water holding-structure in surface layer of the skin, is composed of corneocytes and lamella lipids consisting of ceramides, long chain fatty acid and cholesterols. Corneocytes are covered by cross-linked and cornified envelope and support the epidermal structure. The dermis is a fibrous layer that supports the epidermis and keeps skin elasticity. Dermal connective structures form dense network and contain extracellular matrix (ECM), elastin and collagen fiber, hyaluronic acid (HA), glycosaminoglycans.

Skin aging is mainly classified into two categories: photoaging and chronological aging. Ultraviolet (UV) irradiation is one of the major environmental factors that affects the structure and function of the skin. Long-term exposure to UV radiation, called photoaging, damages both the dermal and epidermal skin and leads to epidermal dryness, thickening (1) and mottled pigmentation (2), laxity (3), and wrinkling (4). Transient strong ultraviolet B (UVB) stimulation initiates an inflammatory response in the epidermis, resulting in the induction of rough skin and barrier dysfunction (5), and reaches to the dermis, resulting in the degeneration of collagenous and elastic fibers which induce a decline in skin elasticity, wrinkle formation, and sagging.

Chronological aging, or so-called “physiological aging,” indicates natural age-induced intrinsic changes. Chronologically aged skin is characterized by dry skin,

atrophy, laxity, and wrinkling. As skin ages, the rate of keratinocyte differentiation slows down, and the reduced cell number induces epidermal thinning and flattening of the epidermal-dermal junction (6, 7) and results in decreased epidermal thickness (8). Loss of natural moisture factors and intercellular lipids such as ceramide cause dry skin, therefore induce reduction of epidermal barrier function (9, 10). Additionally, fibroblast dysfunction and ECM alterations appear in the dermis with aging. Decreases in the content of glycosaminoglycan, proteoglycans, and degeneration of collagenous and elastic fibers induce a decline in skin elasticity, wrinkle formation, and sagging (11).

These skin aging are decreases quality of life remarkably. It has been shown that dietary supplements can contribute to skin health. Oral supplementation with food ingredients, such as vitamins and polyphenols, helps modulate skin function (12-14).

In this study, I focused on two dietary food components: collagen hydrolysate and sphingomyelin (SM). These materials have various physiological activities and recognized useful as dietary beauty and health foods for the skin. Collagen hydrolysate is hydrolyzed product of gelatin derived from fish scale or skin and porcine skin. SM, one of phospholipids, is found in cell membranes as a lipid constituent. Although some studies indicated the improvement of skin function by dietary collagen hydrolysate or SM, their mechanisms remain unclear.

Here, the aim to this study is to investigate effects and mechanisms of dietary collagen hydrolysate and SM on skin aging in molecular level and to utilize food materials for prevention and amelioration of skin aging.

Chapter 1:

Collagen hydrolysate intake improves the loss of epidermal barrier function and skin elasticity induced by UVB irradiation in hairless mice

1-1 Introduction

Collagen is well known as a major constituent of connective tissues including dermis, bone, cartilage, and tendons. It has a characteristic amino acid composition, glycine accounted for 1/3, and contains hydroxyproline (Hyp) as a specific imino acid. Gelatin, a denatured form of collagen that is prepared from animals like fishes, pigs and birds on an industrial scale (15), is popularly used as an additive to foods. Collagen hydrolysate is manufactured from the hydrolysis of gelatin with proteases. Fish derived-collagen hydrolysate is prepared by the procedure as follows; firstly, fish scales and skin are delipidated and removed calcium, and converted to gelatin by heat denaturation. Collagen hydrolysate is prepared by enzymatic hydrolysis of gelatin. Recent reports have shown that nine Hyp-containing peptides, Ala-Hyp, Ser-Hyp-Gly, Ala-Hyp-Gly, Pro-Hyp, Pro-Hyp-Gly, Gly-Pro-Hyp, Ile-Hyp, Leu-Hyp, Phe-Hyp were detected in human plasma, after oral administration of fish scale collagen hydrolysate (16, 17). In particular, Pro-Hyp is identified as the major constituent of collagen hydrolysate. These peptides stimulate chemotaxis (18), cell proliferation (19), and expression of the hyaluronic acid synthase (HAS) gene (20) in human dermal fibroblasts. In addition, collagen hydrolysate intake increases skin collagen expression and suppresses matrix metalloproteinase 2 in normal rats (21). These findings

speculated to whether intake of collagen hydrolysate may have a beneficial effect on UVB-induced decrease in epidermal barrier function and skin elasticity. Recent study reported that collagen ingestion suppressed the decrease of skin hydration and increase of epidermal thickness in hairless mice by UVB irradiation (22). However, there is only limited information on whether collagen hydrolysate intake reduces UVB irradiation-induced loss of epidermal barrier function and skin elasticity in humans or animals. The UVB irradiated animal model has been used for evaluation for protection of skin by cosmetics and foods. Therefore, the objective of the present study in this chapter was to examine the effect of collagen hydrolysate intake on the skin function such as SC water content, transepidermal water loss (TEWL), and skin elasticity after either a single dose or repeated doses of UVB irradiation in hairless mice.

1-2 Methods

Animals

Nine-weeks-old female Hos:HR-1 hairless mice (Japan SLC Inc., Shizuoka, Japan) were housed in plastic cages (4 mice/cage) in a temperature- and humidity-controlled room (24 ± 1ºC and 50 ± 10% humidity) under a 12 h light–dark cycle with a standard AIN-93G diet (Oriental Yeast Co., Ltd, Tokyo, Japan) and water available *ad libitum*. In this study, all of the animal experiments were approved by Meiji Co., Ltd. Institutional Animal Care and Use Committee, and carried out in accordance with the Guiding Principles for the Care and Use of Laboratory Animals approved by Meiji Co., Ltd.

Experiment 1 (single dose of UVB radiation)

The experimental design followed a procedure modified from Hirotsune *et al.* (23)

and Takagi *et al.* (24). Twenty-four mice were randomly divided into three groups (n = 8/group) to show similarly arranged body weight, the SC water content and TEWL. All three groups were given deionized water at 10 ml/kg body weight, and two groups were additionally given protein hydrolysate at 2.0 g/deionized water at 10 ml/kg body; one of these was given fish scale collagen hydrolysate (IXOS HDL-50OH, Nitta Gelatin Inc., Osaka, Japan), and the other was given casein hydrolysate as the control protein hydrolysate. Collagen hydrolysate has an weight average molecular weight of about 5000 Da and casein hydrolysate was hydrolyzed to approximately uniform molecular weight using protease. As shown in Fig 1, mice were given the experimental hydrolysate samples orally for 11 days, from 7 days before UVB irradiation (day -7) until 4 days after irradiation (day 4). At 7 days after initiation of the experimental sample, the dorsal skin was exposed once to 20 mJ/cm^2 of UVB (GL20SE, Sankyo Denki Co., Ltd, Tokyo, Japan) under isoflurane anesthesia. The SC water content and TEWL were measured 7 days before and 0, 1, 2, 3, and 4 days after irradiation. In turn, another set of mice were also orally administered water or collagen hydrolysate at 2.0 g/kg body weight and taken exposure to single UVB irradiation as described above. Four days after irradiation, all mice were sacrificed under isoflurane anesthesia, and all efforts were made to minimize suffering. The dorsal skin was excised quickly and fixed in 10% neutral buffered formalin solution for at least 24 h for histological analysis.

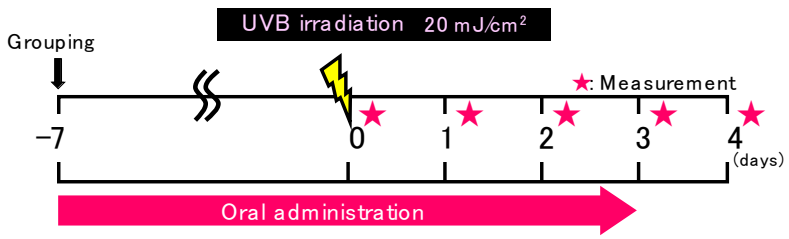

Fig. 1. Experimental scheme of a single dose of UVB irradiation study.

Experiment 2 (repeated doses of UVB radiation)

Twenty mice were assigned randomly to two groups (n = 10/group) according to their body weight, the SC water content, TEWL, and skin elasticity. The control group was fed the control diet (AIN-93G), and the collagen group was fed the collagen diet. It is a mixture containing 2 g of fish scale collagen hydrolysate (IXOS HDL-50OH, Nitta Gelatin Inc., Osaka, Japan) per 100 g of the control diet. The composition of the experimental diets is shown in Table 1. Food intake and body weight were measured once weekly for all groups. After mice had received 1 week of their assigned diet, the dorsal skin of each was exposed to UVB irradiation three times a week for 6 weeks (Fig 2). The doses of UVB per irradiation were increased gradually (25, 26). The dose was set at 10 mJ/cm^2 for the first week (week 1), 15 mJ/cm^2 for the second week (week 2), 20 mJ/cm^2 for the third week (week 3), and 30 mJ/cm^2 for the remaining weeks (week 4-6). The SC water content, TEWL and skin elasticity were measured biweekly. At 6 weeks after initiation of UVB irradiation, all mice were sacrificed under isoflurane anesthesia, and all efforts were made to minimize suffering. The dorsal skin was excised quickly and stored at -80°C until analysis.

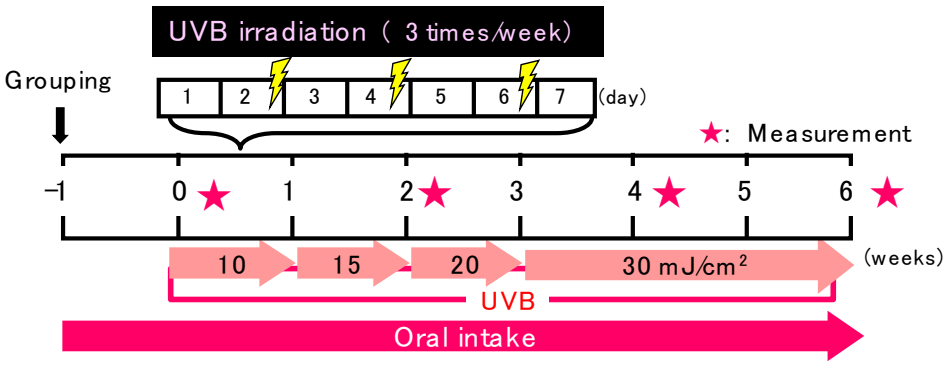

Fig. 2. Experimental scheme of repeated dose of UVB irradiation study.

Table 1. Composition of the experimental diets (Repeated UVB irradiation and intrinsic aging study in chapter 1 and 2)

	Control group	Collagen group
	%	
Casein	20.0	20.0
L-Cystine	0.3	0.3
Collagen hydrolysate	—	2.0
Cornstarch	39.75	39.75
Pregelatinized cornstarch	13.2	13.2
Sucrose	10.0	10.0
Cellulose powder	5.0	5.0
Soybean oil	7.0	7.0
Mineral mixture [1]	3.5	3.5
Vitamin mixture [1]	1.0	1.0
Choline bitartrate	0.25	0.25
tert-Butylhydroquinone	0.0014	0.0014
	100.0	102.0

[1] Reeves *et al.* (27)

Measurement of SC water content and TEWL

The SC water content and TEWL were assessed under standardized conditions (24 ± 1ºC and 50 ± 10% humidity). The SC water content and TEWL were measured with a SKICON 200-EX skin surface hygrometer (IBS Co., Shizuoka, Japan), and a Tewameter MPA580 (Courage and Khazaka Electronic GmbH, Cologne, Germany), respectively.

Measurement of skin elasticity

Skin elasticity was recorded with a Cutometer SEM575 (Courage and Khazaka) as described previous study (25). Measurements were performed in triplicate. The kinetics of skin displacement (2 mm diameter probe) in response to a 2 s of a 300 mbar suction followed by a 2 s relaxation period was measured. The key parameter of skin elasticity

(R2: Ua/Uf), total recovery from deformation divided by total deformation, was calculated from the distension kinetics.

Histological analysis

The dorsal skin sections were stained with hematoxylin and eosin (H&E). The epidermal thickness (the distance from the bottom of the basal layer to the top of the granular layer) was determined with a BX-2 biomicroscope (Olympus, Tokyo, Japan) and a DP-72 CCD camera (Olympus). It was digitally assessed by image measurement and analysis with WinROOF software (Mitani Corporation, Tokyo, Japan). The average of 20 random determinations was considered the representative value for each individual mouse.

Extraction and quantification of dermal hyaluronic acid (HA)

Hyaluronic acid (HA) in the dermis was extracted based on a modified method (28, 29). Approximately 30 mg of full-thickness skin discs were treated with a solution of Dulbecco's modified Eagle's medium containing 0.1% dispase over night at 4ºC and separated into the epidermal- and dermal layer. The separated dermis was frozen and milled in liquid nitrogen (N_2). The powder was recovered in 0.3 ml of a buffer containing Tris (0.1 M) and $CaCl_2$ (4 mM) (pH 8.6). The suspension was centrifuged at 10,000 g for 10 min at 4ºC. The supernatant was decanted, and the pellet was treated with 1.2 ml of chloroform/methanol (2 : 1) and shaken gently for 30 min at room temperature. The suspension was centrifuged at 10,000 g for 20 min at 4 ºC, and the chloroform layer was removed. This procedure was repeated twice. The defatted skin was vacuum-dried for 3 h at 30ºC, and 1 ml of protease from *Streptomyces griseus* (Sigma-Aldrich Japan, Tokyo, Japan) was added. This solution was incubated for 24 h at 50ºC and then boiled for 10 min at 100ºC. The suspension was centrifuged at 14,000

g for 10 min at 4ºC. The supernatant was stored at -80ºC until analysis. Dermal HA quantification was performed by enzyme-linked immunosorbent assay with a hyaluronic acid measurement kit (Seikagaku Corp., Tokyo, Japan).

Statistical analysis

All data in this section are presented as mean standard error (SE). Differences in the data between time zero and each time point were analyzed with Student's paired t-test (SPSS 14.0J, SPSS Inc., Chicago, IL, USA). Differences in the data for the three groups were analyzed by one-way ANOVA, with post hoc analyses being carried out using Tukey's test, while comparisons between the control and collagen groups were performed with Student's t-test. Differences were considered to be significant at $P < 0.05$.

1-3 Results

Experiment 1

The SC water content was significantly lower in all groups on day 1, 2, 3, and 4 after UVB irradiation than on day 0. Collagen hydrolysate administration caused a significant suppression in decrease of the SC water content as compared with control and casein on day 1, 2, 3, and 4 (Fig. 3a). TEWL was significantly higher in the control and collagen groups on day 1, 2, 3, and 4 after irradiation than on day 0. A significant increase in TEWL was observed in the casein group on day 2, 3, and 4 compared with day 0. TEWL suppressed in the collagen group as compared with the control group on day 2, 3, and 4. A significant increase in TEWL was observed in the casein group on day 3 and 4 as compared with the collagen group (Fig. 3b). H&E stained dorsal skin sections and epidermal thickness 4 days after UVB irradiation are shown in Fig. 4a and

b. Remarkable parakeratosis (indicated by the arrow in Fig. 4a), thickening of the prickle-cell layer, and an increase of epidermal cells were observed only in the control group. Epidermal thickness was significantly lower in the collagen group as compared with the control group.

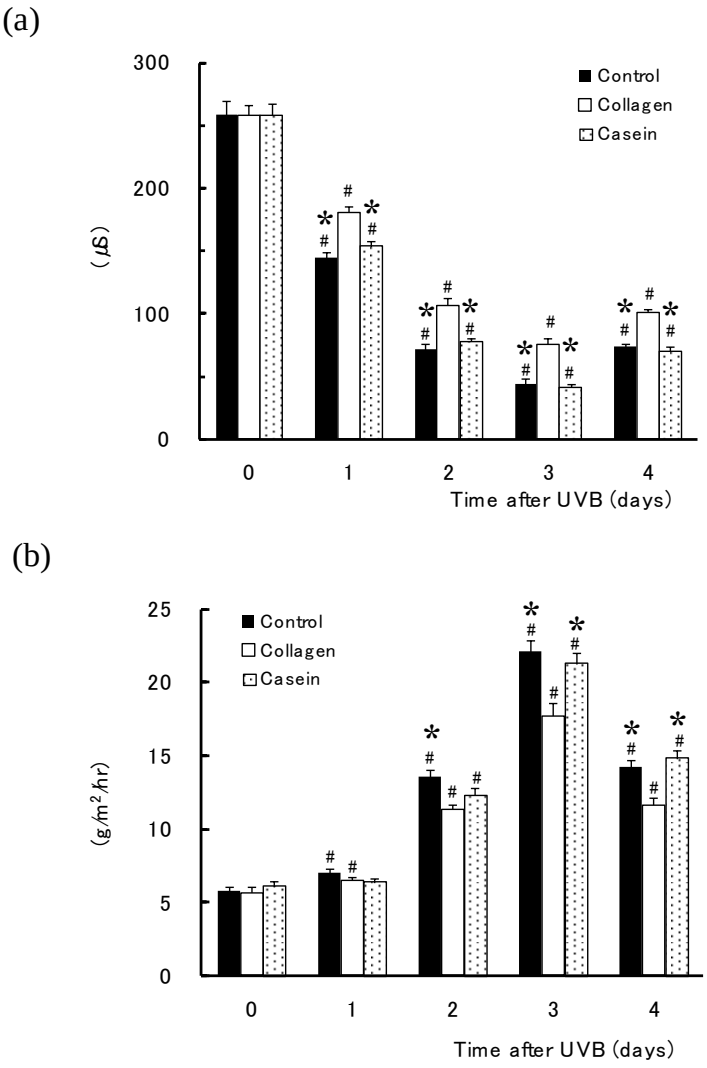

Fig. 3. Effects of collagen hydrolysate administration on and SC water content (a) and TEWL (b) after a single dose of UVB irradiation.

The values are shown as mean ±SE (n=8). *$P < 0.05$ (vs. the collagen group). #$P < 0.05$ (vs. day 0).

(a)

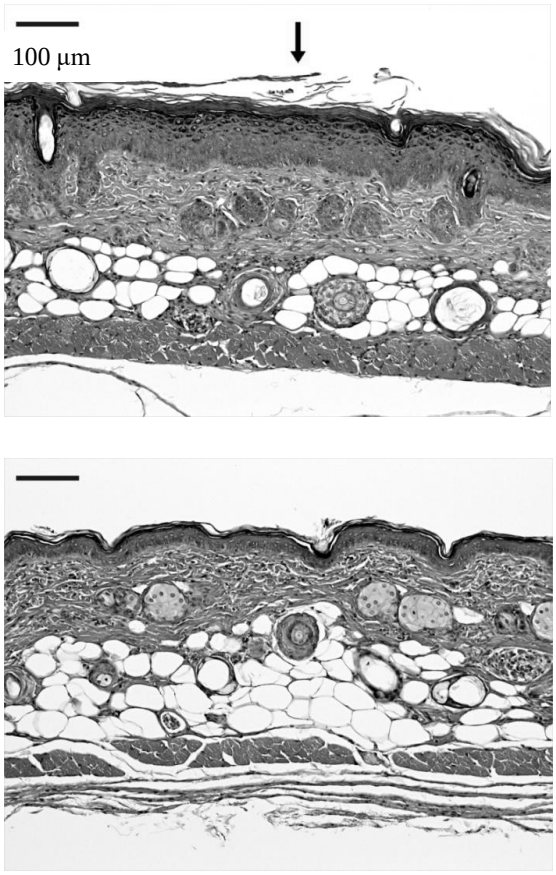

(b)

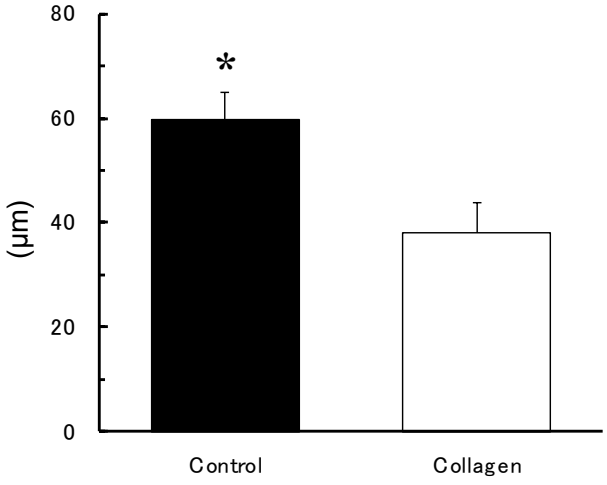

Fig. 4. H&E-stained dorsal skin tissue sections (a) and epidermal thickness (b).

The Epidermal thickness value 4 days after UVB irradiation are shown as mean ± SE (n = 8). *$P < 0.05$ (vs. the collagen group).

Experiment 2

Body weight and food intake were similar between groups during the experiment (data not shown). Each mouse in the collagen group was fed 2.56 ± 0.03 g/kg body weight/day of collagen hydrolysate. The changes of SC water content and TEWL are shown in Fig. 5a and b. The SC water contents of both groups at all time points after initiation of UVB irradiation were significantly lower than at week 0 (Fig. 5a). Collagen ingestion significantly increased the water content at week 2, 4, and 6 compared to control group. TEWL was significantly higher in the control group at week 2, 4, and 6 than at week 0 (Fig. 5b). A significant increase in TEWL was found in the collagen group at week 4 and 6 compared with week 0. TEWL was significantly lower in the collagen group than in the control group at week 4 and 6. Skin elasticity is shown in Fig. 5c. The R2 value was significantly lower in the control group at all time points after initiation of irradiation than at week 0, while the value in the collagen group at week 2 was significantly lower than at week 0. Skin elasticity increased significantly in the collagen group compared with the control group at week 6. Dermal HA content 6 weeks after initiation of UVB irradiation is shown in Fig. 6. HA content was significantly higher in the collagen group than in the control group.

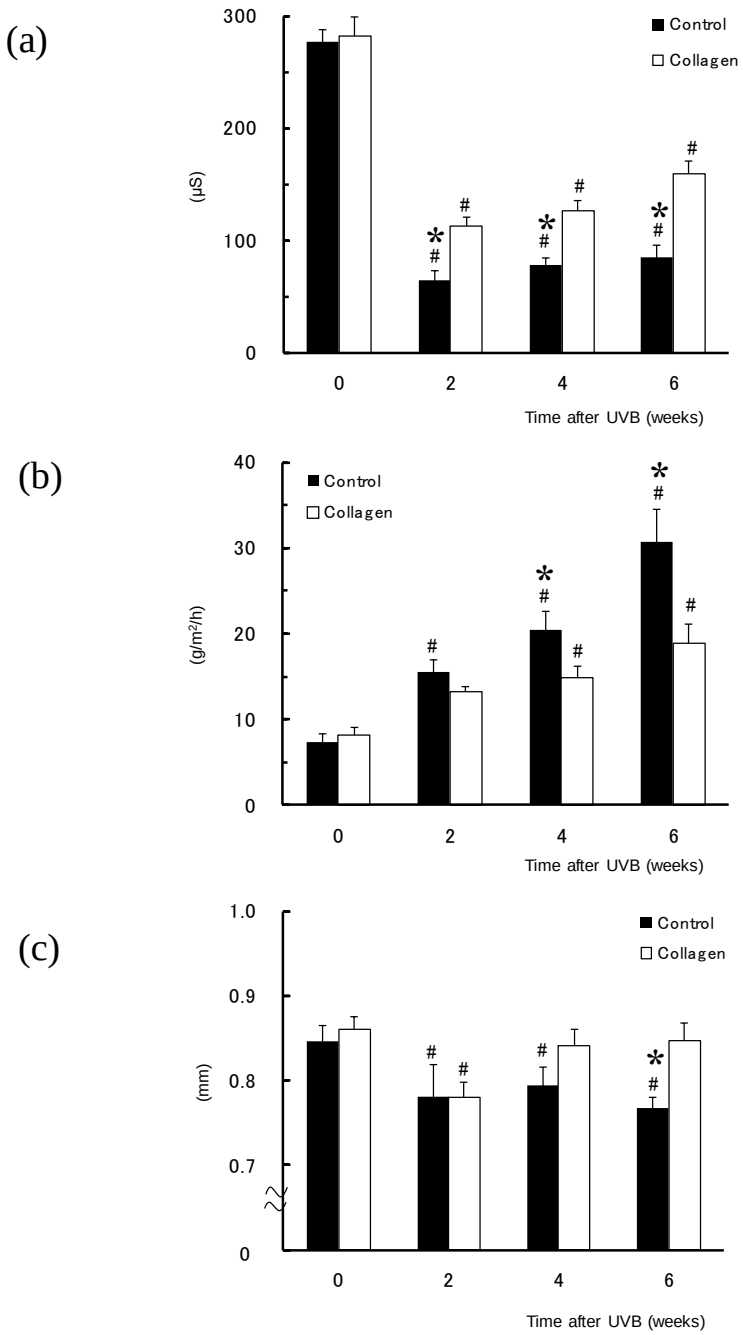

Fig. 5. Effect of collagen hydrolysate on the SC water content (a), TEWL (b), and skin elasticity (c) after repeated irradiation with UVB.

The values are shown as mean ± SE (n = 10). **P* < 0.05 (vs. the collagen group). #*P* < 0.05 (vs. day 0).

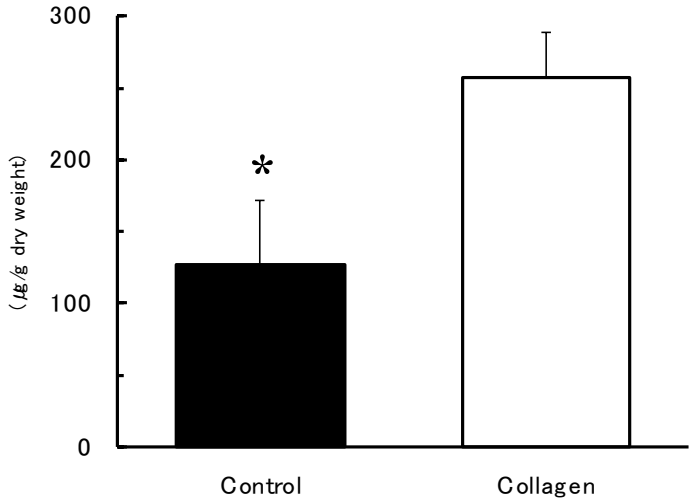

Fig. 6. Hyaluronic acid (HA) content in the dermis 6 weeks after initiation of UVB irradiation.

The values are shown as mean ± SE (n = 10). *$P < 0.05$ (vs. the collagen group).

1-4 Discussion

In this chapter, I evaluated the effect of collagen hydrolysate ingestion on skin damaged by UVB irradiation, especially on the epidermal barrier and on dermal elasticity defects, in hairless mice. I showed for the first time that the ingestion of collagen hydrolysate significantly reduced UVB irradiation induced abnormality on both epidermal barrier and skin elasticity. A single dose of UVB irradiation significantly decreased SC water content and increased TEWL. In addition, in this animal model, epidermal hyperplasia was observed 4 days after a single dose of UVB irradiation. Haratake *et al.* (30) also observed a barrier alteration 72 h after UVB irradiation in hairless mice. This delay in the barrier abnormality depends on cellular or metabolic changes in underlying skin layers. This earlier study also showed that UVB exposure increases DNA synthesis and prostaglandin E2 levels as a consequence of epidermal hyperplasia. Furthermore, the UVB-induced barrier defect was linked to a

hyperproliferative response in epidermal keratinocytes. Tanaka *et al.* (22) found the same effects after repeated irradiation. The present study demonstrated that dietary collagen hydrolysate significantly suppressed not only the decrease in the SC water content and increase in TEWL after a single dose of UVB irradiation but also the resulting epidermal hyperplasia. It is possible, therefore, that intake of collagen hydrolysate suppresses UVB irradiation induced proliferative responses in the SC, although the mechanism of this action remains unclear. Furthermore, the current study also demonstrates that ingestion of the collagen hydrolysate reduces the loss of epidermal barrier function and skin elasticity induced by repeated UVB irradiation and suppresses the HA content in dermis. It is possible that dermal HA may have an important role in both epidermal barrier function and skin elasticity. Chronic UVB exposure can result in alterations in dermal structure and elasticity (25, 31). The elasticity is closely associated with the dermal components, especially the ECM. The ECM is a dense meshwork of collagen and elastin, embedded in a viscoelastic ground substance composed of proteoglycans and glycoproteins, such as HA (32). It has been shown that skin exposure to chronic UVB irradiation damages the basement membrane and decreases the dermal HA content, owing to the suppression of HAS mRNA expression (33). Therefore, increasing dermal HA content may reduce the UVB induced degradation of dermal matrix components, thereby increasing skin elasticity in mice fed collagen hydrolysate. HA also acts as a kind of huge water storage system; it is essential for maintaining skin water retention as well as skin elasticity. In the recent study, it has been demonstrated that exogenous HA plays a beneficial role by interacting with fibroblasts to enhance epidermal morphogenesis, improving basement membrane assembly and formation of the epidermal lipid barrier in an organotypic

keratinocyte–fibroblast coculture model (34). Okawa *et al*. (35) also reported that collagen hydrolysate intake increased the expression of HAS genes as a consequence of a reduction in acetone-induced skin dryness in model mice. Thus, suppression of decreasing in dermal HA may have a beneficial role in epidermal homeostasis, resulting in an increase in SC water content. It is known that collagen has a high concentration of Hyp compared with other dietary protein sources. Previous reports showed that not only amino acids but also di- and tripeptides, such as Pro-Hyp, Ala-Hyp, and Pro-Hyp-Gly, were detected in human blood after the intake of collagen hydrolysate (16, 17). The major dipeptide, Pro-Hyp, induced cell proliferation and HA synthesis in human dermal fibroblasts (20). Maximal stimulation of cell proliferation and HAS by Pro-Hyp was achieved at doses of 200 nmol/mL, which is similar to physiological concentrations because the concentration of collagen-derived Hyp containing peptides in plasma 2 h after orally collagen hydrolysate at 25 g/65 kg body weight/man is reported to be approximately 140 nmol/mL human plasma. Furthermore, preliminary study also showed that the peak concentration of collagen-derived Hyp-containing peptides in mouse plasma was the same level as in human plasma (data not shown). In addition, orally administered [^{14}C]Pro-Hyp was distributed in skin partly as the intact form in rats (36). It is possible, therefore, that the active components in collagen hydrolysate stimulated dermal fibroblasts and activated signaling for HA synthesis, resulting in an increase in dermal HA content.

In summary, the results in this chapter demonstrated that repetitive collagen hydrolysate administration is not only skin barrier abnormalities but also skin elasticity dysfunction induced UVB irradiation.

Chapter 2:

Effect of orally administered collagen hydrolysate on gene expression profiles in mouse skin: a DNA microarray analysis

2-1 Introduction

Although some studies described the effect of collagen hydrolysate administration on the skin (37, 38, 39), there is no description or comprehensive analysis of how long-term administration of collagen hydrolysate affects gene expression associated with skin barrier function and elasticity under conditions of intrinsic aging. DNA microarray technology can analyze comprehensively the expression of many genes and find several novel markers associated with physiological functions. It is an effective approach to understand how food ingredients affect gene expression in target tissues (40, 41). In this section, I evaluated the SC water content and skin elasticity and applied DNA microarray analysis to investigate novel effects of long-term administration of collagen hydrolysate on the aged skin.

2-2 Methods

Animals

Nine-weeks-old female Hos:HR-1 hairless mice (Japan SLC, Shizuoka, Japan) were used in this study. As described in chapter 1-2, all mice were housed in plastic cages in a temperature- and humidity-controlled room under a 12 h light-dark cycle with a standard AIN-93G diet and water available *ad libitum*. All of the animal experiments were approved by the Animal Committee of Meiji Seika Kaisha, Food & Health R&D

Laboratories, with the animals receiving care under the Guiding Principles for the Care and Use of Laboratory Animals of the committee.

Experiment 1 (skin evaluation in an aging mouse model)

After acclimatization for 3 days, sixteen mice were randomly divided into two groups (n = 8/group) according to their body weight, SC water content, and skin elasticity. During the experimental period for 12 weeks, the control group was fed a control diet (AIN-93G) and the collagen group was fed a collagen diet consisting of a mixture of 2.0 g of fish scale collagen hydrolysate (IXOS HDL-50OH, Nitta Gelatin Inc., Osaka, Japan) and 100 g of the control diet. This amount of collagen hydrolysate is approximately equivalent to oral ingestion of 2.0 g collagen hydrolysate/kg body weight/day on UVB irradiation study as discussed in the chapter 1-2. The composition of the experimental diets is shown in Table 1. Food intake and body weight were measured once a week in all groups. The SC water content and skin elasticity were measured once every 2 weeks. The measurement data are presented as means ± SE. The skin parameters, SC water content and skin elasticity were assessed under standardized conditions as described in previous chapter 1-2. Differences in the data between time zero and each time point were analyzed with a Student's paired t-test (IBM SPSS statistics 22.0; SPSS, Chicago, IL), while comparisons between the control and collagen groups were performed with a Student's t-test. Differences were considered to be significant when $P < 0.05$.

Experiment 2 (Microarray analysis of skin)

Sixteen mice were divided into two groups (n = 8/group) after acclimatization for 3 days. The control group was fed a control diet (AIN-93G) and the collagen group was fed a collagen diet (fish scale collagen hydrolysate added AIN-93G) as described in

experiment 1. After 12 weeks administration of the experimental diet, all mice were sacrificed under isoflurane anesthesia, and all efforts were made to minimize suffering. The dorsal skin was excised quickly and stored in RNAlater (Applied Biosystems, Foster City, CA) at -80ºC. Additionally, for comparison at 1 week after administration, sixteen female mice were divided into the control and the collagen group (n = 8/group) and gave them the experimental diet as described above. At 1 week after administration, the skin of all individuals was collected as above.

Isolation of total RNA

Dorsal skin samples of each mouse were frozen in liquid N_2 and powdered using a mortar and pestle. Total RNA was isolated from the samples with TRIzol reagent (Life Technologies, Carlsbad, CA) and chloroform (Wako Pure Chemical Industries, Osaka, Japan) and purified with the RNeasy Mini Kit (Qiagen, Hilden, Germany). The quality and quantity of total RNA were spectrophotometrically evaluated with an Agilent 2100 Bioanalyzer (Agilent Technologies, Santa Clara, CA) and an RNA 6000 Nano Series II Kit (Agilent Technologies). A RNA integrity number (RIN) was computed with 2100 Expert Software (Agilent Technologies) to indicate the integrity of total RNA samples on a scale of 1–10 (42). The RIN of total RNA isolated from each skin sample was > 9.0.

DNA microarray assay

From each group, four mice, who had a SC water content close to the average level, were selected. Total RNA samples from individuals were subjected to DNA microarray analysis as described previously (43). In brief, using a GeneChip 3'IVT Express Kit (Affymetrix, Santa Clara, CA), complementary DNA (cDNA) was synthesized from 200 or 300 ng purified total RNA, and biotinylated amplified RNA (aRNA) was

transcribed with T7 RNA polymerase. The aRNA was fragmented and hybridized to an Affymetrix GeneChip Mouse Genome 430 2.0 Array (Affymetrix), which contained probes for > 39,000 mouse genes. After hybridization at 45°C for 16 h, the array was washed and stained with phycoerythrin. Fluorescence signals were scanned with the Affymetrix GeneChip System (Affymetrix). To reduce array images to the intensity of each probe, affymetrix GeneChip Command Console software (Affymetrix) was used. All the microarray data are MIAME compliant and have been deposited in a MIAME compliant database, the National Center for Biotechnology Information Gene Expression Omnibus (GEO) (http://www.ncbi.nlm.nih.gov/geo/, GEO Series accession number GSE62650), as detailed on the MGED Society website (http://fged.org/projects/miame/). The raw microarray data (CEL files) were quantified with the "distribution free weighted" method (DFW) (44), using the statistical language R (45) and Bioconductor (46). Hierarchical clustering was then performed using the pvclust function (47) in R. To identify differentially expressed genes between groups, the rank products method (48) was applied to the DFW quantified data. Probe sets with Benjamini and Hochberg false discovery rate (FDR) (49) corrected P value < 0.05 were regarded as having different expression levels between groups according to previous microarray studies (50). The annotation file for the Mouse Genome 430 2.0 Array was downloaded from the Affymetrix Web site (http://www.affymetrix.com/). The selected probe sets were functionally classified according to "biological process" in Gene Ontology (GO) with the functional annotation tool of the Database for Annotation, Visualization, and Integrated Discovery (DAVID) (51). The probe set IDs provided by Affymetrix were used as the input data format. For the gene list manager on the DAVID web site (http://david.abcc.ncifcrf.gov/), the species option to limit annotations

exclusively to Mus musculus were selected. Gene annotation enrichment analysis of differentially expressed genes was performed by the DAVID functional annotation tool on the basis of GOTERM_BP5 in GO biological process. A P value < 0.05 indicated a significantly enriched GO term. To visualize the hierarchical structure of selected GO terms, I used QuickGO (52) (https://www.ebi.ac.uk/QuickGO/), an online analysis utility.

cDNA synthesis and quantitative real-time reverse transcription polymerase chain reaction analysis

For cDNA synthesis from extracted total RNA, reverse transcription was performed using a RevertAid First Strand cDNA Synthesis Kit (Thermo Fisher Scientific, Waltham, MA). Quantitative Real-time polymerase chain reaction (PCR) was performed using the ABI 7500 Fast Realtime PCR system (Applied Biosystems). The respective primers and probes (TaqMan Gene Expression Assays) were designed at Applied Biosystems from gene sequences obtained from GenBank (aquaporin 3: Mm01208559_m1, involcrin: Mm00515219_s1, desmoglein 1 beta: Mm00839130_mH, glyceraldehyde-3-phosphate dehydrogenase [GAPDH]: Mm99999915_g1). The relative expression of the gene of interest was normalized relative to GAPDH mRNA levels and then calculated by the $2^{-\Delta\Delta Ct}$ method (53). The results are expressed as arbitrary units. The measurement data are expressed as fold changes ± SE. The gene expression data were analyzed with Student's t-test at the ΔCt stage to exclude potential bias due to the averaging of data transformed through the equation $2^{-\Delta\Delta Ct}$ (54). Differences among groups were considered to be significant at $P < 0.05$.

2-3 Results

Experiment 1

Body weight and food intake showed no significant differences between the two groups (data not shown). Each mouse in the collagen group was fed 2.51 ± 0.03 g collagen hydrolysate/kg body wt/day. The SC water content is shown in Fig. 7a. The SC water content in the control group was significantly lower at week 4, 6, 8, 10, and 12 than week 0. In the collagen group, water content was significantly higher at week 2, 4, 6, 8 and lower at week 10 than week 0. Twelve weeks of oral administration of collagen hydrolysate showed significantly higher values in SC water content compared with the control group at week 4, 6, 8, 10, and 12. Skin elasticity data are shown in Fig. 7b. The R2 value was significantly lower in the control group at week 12 than week 0, while no significance was found in the collagen group. Skin elasticity was significantly higher in the collagen group compared with the control group at week 4, 6, 8, 10, and 12.

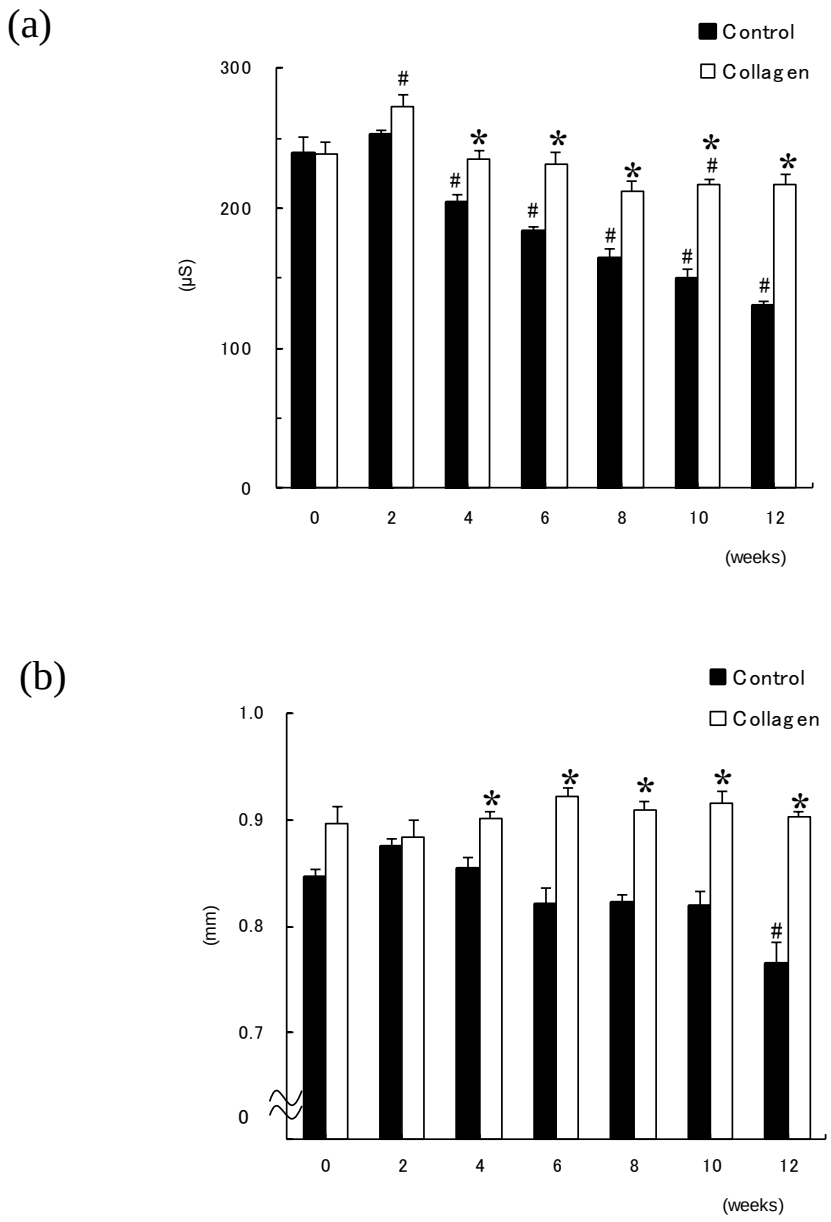

Fig. 7. Effect of collagen hydrolysate on SC water content and skin elasticity over time.

The values of SC water content (a) and skin elasticity (b) are shown as means ± SE (n = 8). *$P < 0.05$ (vs. the control group). #$P < 0.05$ (vs. day 0).

Experiment 2

Comparison at 12 weeks after administration

After 12 weeks collagen hydrolysate administration, body weight and food intake showed no significant differences between the two groups (data not shown). Each mouse in the collagen group was fed 2.67 ± 0.02 g collagen hydrolysate/kg body wt/day. The DFW quantified microarray data was subjected to hierarchical clustering analysis to evaluate overall gene expression profiles. The cluster dendrogram revealed that each experimental group was not clustered (Fig. 8a). This result indicates that there were no significant differences in gene expression profiles in the skin following collagen hydrolysate administration for 12 weeks. Consequently, extraction of differentially expressed genes (DEGs) and GO analysis were not performed.

Comparison at 1 week after administration

There were no significant changes in body weight or food intake between the groups after 1 week oral administration of collagen hydrolysate (data not shown). Each mouse in the collagen group was fed 2.91 ± 0.01 g collagen hydrolysate/kg body wt/day. Hierarchical clustering analysis revealed that DFW quantified microarray data of each group formed a distinct cluster, indicating that the gene expression profiles differed between the collagen group and the control group (Fig. 8b). This result suggests that 1 week of collagen hydrolysate administration changed the gene expression patterns in the skin. Applying a significance value for FDR of < 0.05, 155 upregulated probe sets (135 genes) and 528 downregulated probe sets (448 genes) in the collagen group compared with the control group were identified. DEGs were classified into functional categories by the GO biological process annotation. The significantly enriched GO terms (P <

0.05) for the gene sets that were up- and down-regulated by collagen hydrolysate intake are summarized in Tables 2 and 3, respectively. In the upregulated gene set, these include GO terms related to “developmental process,” “metabolic process,” “biological regulation,” “response to stimulus,” and “single-organism process.” “Immune system process,” “response to stimulus,” “developmental process,” “single organism process,” “biological regulation,” and “metabolic process” are GO terms enriched in the downregulated gene set. Gene annotation enrichment analysis (as above) is able to detect only those genes with the same GO annotation that are statistically enriched in a given population of DEGs. To complement the GO analysis, DEGs related to skin, especially function and structure in the epidermis and dermis, were selected (Tables 4 and 5). Among fibrous structural proteins, the keratin family was differentially expressed in response to collagen hydrolysate intake. Type II cytokeratin, keratin 2 (Krt2), and keratin 6B (Krt6b) were up-regulated, while other keratin family genes in the epidermis were downregulated in the collagen group. Epiregulin (Ereg), epidermal growth factor, and aquaporin 3 (Aqp3), a water channel in the epidermis, were upregulated in the collagen group. Furthermore, cornified envelope (CE) and corneodesmosome-related DEGs that were upregulated in the collagen group include repetin (Rptn), involucrin (Ivl), small proline-rich protein 1B (Sprr1b), stefin A2-like 1 (Stfa2l1), and desmoglein 1B (Dsg1b). Dermal ECM-related genes appear in the collagen group. Matrix metallopeptidases-9 (Mmp9), -11 (Mmp11), -13 (Mmp13), -19 (Mmp19), and heparanase (Hpse), which are enzymes responsible for degradation of the ECM and basement membrane, were down-regulated in the collagen group. Conversely, certain components of the ECM including chondroitin sulfate proteoglycan-4 (Cspg4), fibronectin-1 (Fn1), and proteoglycan-4 (Pg4) were upregulated in the collagen group.

To confirm result of the DNA microarray analysis, quantitative real-time reverse transcription polymerase chain reaction (qRT-PCR) was applied to three selected genes associated with keratinocyte (Aqp3) and CE and corneodesmosome-related DEGs (Ivl and Dsg1b). The expression levels of these genes exhibited significant increases in the collagen group compared with control group (Fig. 9a, b, c).

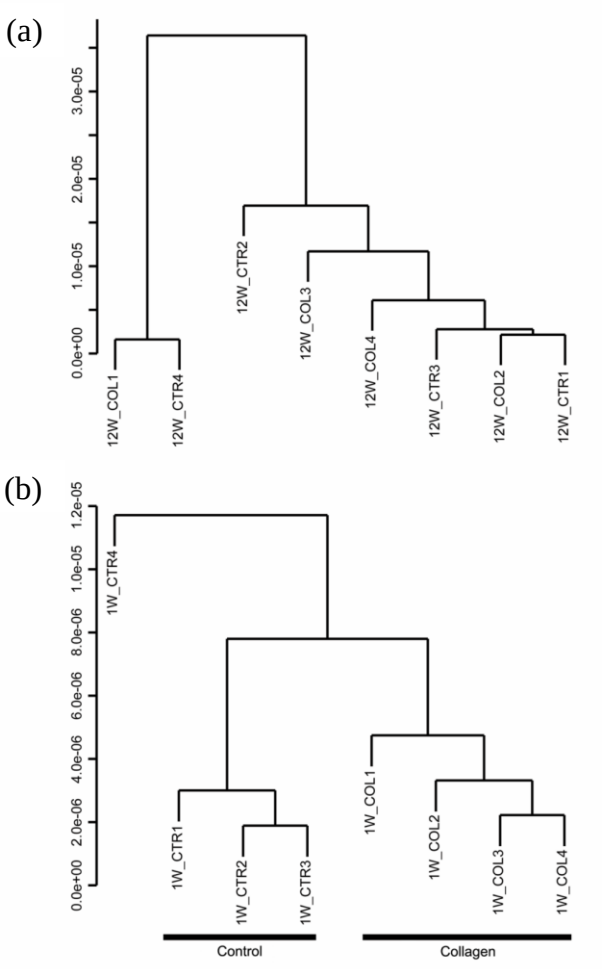

Fig. 8. Hierarchical clustering dendrogram of distribution free weighted (DFW)-quantified microarray data after 12 weeks and 1 week of administration of collagen hydrolysate.

Cluster dendrograms after 12 week (a) and 1 week (b) of administration of collagen hydrolysate are shown. The vertical scale represents the distance between clusters. Each name comprises a letter and a number corresponding to the individual mouse as follows: 12W_CTR 1– 4: Control group at 12 weeks after administration; 12W_COL 1– 4: Collagen group at 12 weeks after administration; 1W_CTR 1– 4: Control group at 1 week after administration; 1W_COL 1– 4: Collagen group at 1 week after administration.

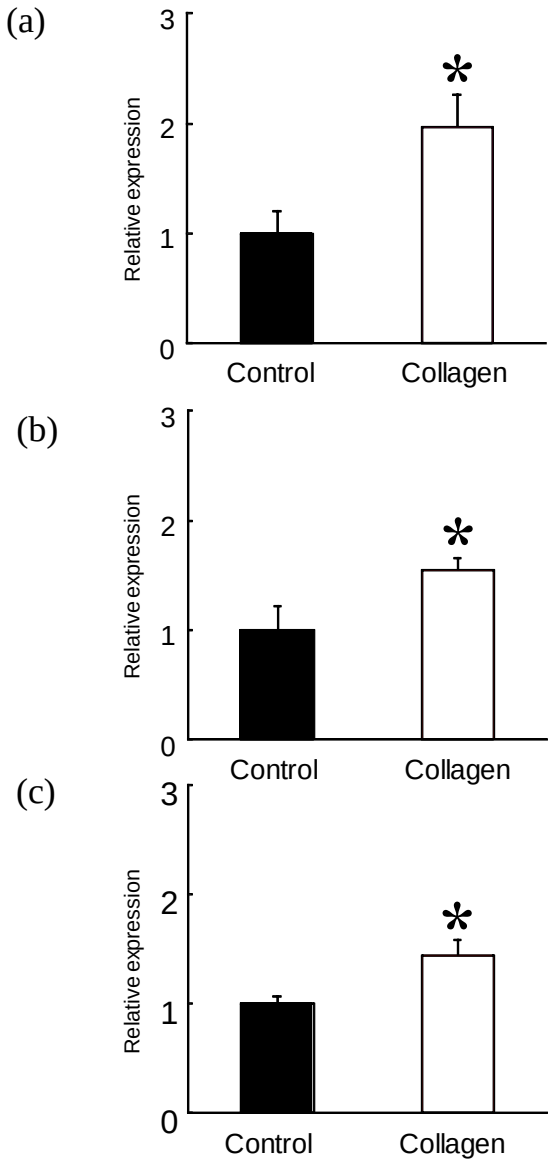

Fig. 9. Effect of collagen hydrolysate on Aquaporin 3 (Aqp3), Involucrin (Ivl), and desmoglein 1 beta (Dsg1b) mRNA expression.

Aqp3 (a), Ivl (b), and Dsg1b (c) mRNA levels are shown as fold-changes ± SE (n = 8). *$P < 0.05$ (vs. the control group).

Table 2. Significantly enriched GO terms ($P < 0.05$) identified among the gene set up-regulated by collagen hydrolysate intake.

GO-ID	GO Term	*p*-value
	developmental process	
0009888	tissue development	3.33E-03
0060429	epithelium development	3.49E-02
0009913	epidermal cell differentiation	4.55E-02
0031424	Keratinization	1.49E-02
0001944	vasculature development	2.59E-02
0001568	blood vessel development	2.36E-02
0009887	organ morphogenesis	1.73E-02
	metabolic process	
0006694	steroid biosynthetic process	1.19E-02
0016126	sterol biosynthetic process	1.70E-02
0006695	cholesterol biosynthetic process	1.02E-02
0009072	aromatic amino acid family metabolic process	8.53E-03
0019752	carboxylic acid metabolic process	1.29E-03
0046394	carboxylic acid biosynthetic process	1.46E-02
0006631	fatty acid metabolic process	7.72E-03
0006633	fatty acid biosynthetic process	2.09E-03
0006583	melanin biosynthetic process from tyrosine	1.33E-02
0006720	isoprenoid metabolic process	4.24E-02
	biological regulation	
0045934	negative regulation of nucleobase, nucleoside, nucleotide and nucleic acid metabolic process	4.94E-02
0016481	negative regulation of transcription	3.80E-02
	response to stimulus	
0006935	Chemotaxis	7.90E-06
	single-organism process	
0016477	cell migration	5.34E-03
0050900	leukocyte migration	3.34E-02

Table 3. Significantly enriched GO terms ($P < 0.05$) identified among the gene set down-regulated by collagen hydrolysate intake.

GO-ID	GO Term	*p*-value
	immune system process	
GO:0002449	lymphocyte mediated immunity	1.21E-05
GO:0019724	B cell mediated immunity	3.25E-06
GO:0050778	positive regulation of immune response	5.11E-05
GO:0002253	activation of immune response	1.16E-03
GO:0006956	complement activation	5.30E-04
GO:0006958	complement activation, classical pathway	2.28E-03
	response to stimulus	
GO:0002526	acute inflammatory response	2.04E-05
GO:0006935	Chemotaxis	1.69E-02
	developmental process	
GO:0060323	head morphogenesis	2.77E-02
GO:0009888	tissue development	4.11E-04
GO:0007398	ectoderm development	1.29E-02
GO:0060537	muscle tissue development	5.11E-05
GO:0014706	striated muscle tissue development	2.71E-05
GO:0048738	cardiac muscle tissue development	4.28E-03
GO:0008544	epidermis development	9.35E-03
GO:0043588	skin development	1.84E-02
GO:0001942	hair follicle development	1.43E-02
GO:0031069	hair follicle morphogenesis	5.10E-03
GO:0009887	organ morphogenesis	1.68E-02
GO:0048730	epidermis morphogenesis	8.83E-03
GO:0007507	heart development	1.05E-03
GO:0048534	hemopoietic or lymphoid organ development	4.02E-02
GO:0030097	hemopoiesis	2.05E-02
GO:0007517	muscle organ development	1.14E-06
GO:0060538	skeletal muscle organ development	1.27E-02
GO:0001944	vasculature development	2.77E-03
GO:0001568	blood vessel development	6.50E-03
GO:0010927	cellular component assembly involved in morphogenesis	2.98E-02
GO:0030239	myofibril assembly	5.10E-03
GO:0055001	muscle cell development	9.75E-04
GO:0055002	striated muscle cell development	5.06E-04
GO:0051146	striated muscle cell differentiation	6.61E-03
GO:0060348	bone development	2.40E-02
	single-organism process	
GO:0031032	actomyosin structure organization	1.12E-02
GO:0045214	sarcomere organization	1.73E-02
GO:0015671	oxygen transport	1.73E-02
GO:0006941	striated muscle contraction	9.95E-03
	biological regulation	
GO:0045597	positive regulation of cell differentiation	4.74E-02
GO:0043269	regulation of ion transport	2.92E-02
GO:0010959	regulation of metal ion transport	1.25E-02
GO:0006937	regulation of muscle contraction	4.16E-02
	metabolic process	
GO:0019318	hexose metabolic process	1.46E-02
GO:0006006	glucose metabolic process	4.97E-03
GO:0051604	protein maturation	4.46E-04
GO:0016485	protein processing	1.52E-03
GO:0030574	collagen catabolic process	2.40E-04

Table 4. Up- and down-regulation of epidermal function and structure-related genes in the skin of mice with collagen hydrolysate administration (FDR < 0.05)

	Probe set ID	Gene Title	Gene Symbol	Up/Down	FDR
Keratinocyte	1422588_at	keratin 6B	*Krt6b*	Up	0
	1427154_at	keratin 2	*Krt2*	Up	0
	1419431_at	epiregulin	*Ereg*	Up	0.029350
	1422008_a_at	aquaporin 3	*Aqp3*	Up	0.010364
	1418173_at	keratin 25	*Krt25*	Down	0.041247
	1418742_at	keratin 34	*Krt34*	Down	0
	1421589_at	keratin 31	*Krt31*	Down	0.020488
	1427179_at	keratin 33B	*Krt33b*	Down	0.003500
	1427365_at	keratin 86	*Krt86*	Down	0.000526
	1430132_at	keratin 28	*Krt28*	Down	0.016345
	1436160_at	keratin 26	*Krt26*	Down	0.016401
	1436557_at	keratin 73	*Krt73*	Down	0.034000
	1448457_at	keratin 71	*Krt71*	Down	0.008378
	1449378_at	keratin 27	*Krt27*	Down	0.016871
	1449387_at	keratin 33A	*Krt33a*	Down	0.000185
	1460185_at	keratin 83	*Krt83*	Down	0.024741
Cornified envelope (CE) and Corneodesmosin	1420431_at	repetin	*Rptn*	Up	0
	1422222_at	involucrin	*Ivl*	Up	0.014714
	1439878_at				0.044615
	1422672_at	small proline-rich protein 1B	*Sprr1b*	Up	0.002439
	1442339_at	stefin A2 like 1	*Stfa2l1*	Up	0.046522
	1419709_at	stefin A3	*Stfa3*	Down	0.041711
	1455519_at	desmoglein 1 beta	*Dsg1b*	Up	0.043742
	1435191_at	corneodesmosin	*Cdsn*	Down	0.023019

Table 5. Up- and down-regulation of dermal function and structure-related genes in the skin of mice with collagen hydrolysate administration (FDR < 0.05).

	Probe set ID	Gene Title	Gene Symbol	Up/Down	FDR
Extracellular matrix	1416298_at	matrix metallopeptidase 9	*Mmp9*	Down	0.041343
	1417234_at	matrix metallopeptidase 11	*Mmp11*	Down	0.017085
	1417256_at	matrix metallopeptidase 13	*Mmp13*	Down	0.007178
	1421977_at	matrix metallopeptidase 19	*Mmp19*	Down	0.006172
	1433930_at	heparanase	*Hpse*	Down	0.034207
	1423341_at	chondroitin sulfate proteoglycan 4	*Cspg4*	Up	0.035077
	1437218_at	fibronectin 1	*Fn1*	Up	0.000968
	1449824_at	proteoglycan 4	*Prg4*	Up	0

2-4 Discussion

In this chapter, I found that long-term intake of collagen hydrolysate improved skin condition. Epidermal barrier and dermal elasticity dysfunctions were chronologically induced by aging in the hairless mouse. These damages in the collagen hydrolysate administered group were significantly suppressed 2 weeks after starting administration and a positive long-lasting effect was observed at week 12. However, there were no significant differences of gene expression between groups in week 12. Thus, I considered that one possibility that the determinants for physiological changes, namely gene expression, are altered at an early stage of this experiment because Marshall *et al.* (55) reported that the gene induction pattern of SC precursors such as Sprr1 precedes development of barrier function in terminally differentiating epithelium. In present study, the microarray data at 1 week after administration show that the gene expression profile of the collagen intake group was significantly different from that of the control group. These findings suggest that significant changes of gene expression in the skin precede alteration of SC water content and skin elasticity. Additionally, previous *in vitro* study shows that gene changes of dermal fibroblasts treated with collagen-derived peptides appeared at intervals of 6 h (20). Therefore, expression of genes related to *in vivo* skin function changes might occur at short time interval similarly, but further analyses are required to unravel relation between changes in gene expression and function in the skin.

There is a possibility that oral administration of collagen hydrolysate improves skin dysfunction through alteration of gene expression in the skin. Interestingly, in the present study, GO analysis reveals that GO terms related to “developmental process,” especially epidermal development, were significantly enriched among upregulated

genes after collagen hydrolysate administration. Based on these results, I hypothesize that oral administration of collagen hydrolysate facilitated proliferation and differentiation (i.e., turnover) of skin cells. Since it is known that decreased cell turnover is caused by chronological aging (56), there is the possibility that skin aging is suppressed by promoting functional and structural changes of the epidermis and dermis. Therefore, I focused on up- or downregulated genes related to epidermal and dermal function and structure, with particular emphasis on epidermal proliferation and differentiation.

Genes that directly contribute to the promotion of proliferation and differentiation of keratinocytes, including Ereg (57), Rptn (58), Ivl (59), Sprr1b (60), and Stfa2l1 (61), were significantly upregulated by collagen hydrolysate administration. These results suggest that administered collagen hydrolysate enhanced epidermal turnover. It is important that corneocytes are arranged with regularity in the SC to hold water content in the epidermis (62). The keratinocyte differentiation-associated genes (Rptn, Ivl, Sprr1b, Stfa2l1) encode precursor proteins of the CE, which is a hydrophobic structure formed beneath the plasma membrane of corneocytes in the SC (58, 63). Similarly, expression of the cell adhesion molecule Dsg1b, which is a constituent of junctions between corneocytes (64), was upregulated by collagen administration. Upregulation of Ivl and Dsg1b at the mRNA level by qRT-PCR also were confirmed. Therefore, I consider that collagen hydrolysate enhanced structure of the SC and suppressed epidermal water loss.

In addition, it is also worth noting that Aqp3, a membrane transporter of water and glycerol in the basal layer of epidermal keratinocytes (65, 66), was upregulated by collagen hydrolysate administration. It was also reproducible at the mRNA level.

Recent studies have shown that Aqp3 gene expression in the epidermis is decreased by chronological aging (67), and SC hydration and elasticity were reduced in Aqp3-deficient mice compared with wild-type mice (68). Taken together, these previous works suggest a possibility that upregulation of Aqp3 by collagen hydrolysate is one of the major reasons for improvement of skin barrier function. I suggested that collagen-derived peptides positively regulate epidermal water content through upregulation of genes such as Aqp3. In fact, it has been reported that aquaporins in the skin play an important role in the maintenance of homeostasis and enhance wound healing (68). However, the changes of Aqp 3 gene expression in this study is found in full-thickness skin, thus further consideration will be needed about expression of epidermis-localized Aqp 3 genes.

I found that collagen administration caused facilitation of epidermal proliferation and differentiation, maintenance of structure in the SC, and regulation of water channels at the gene expression level. It is also suggested that these gene alterations are accompanied by changes in phenotype such as SC water content. Therefore, it is concluded that activation of these genes in the epidermis is important to maintain epidermal barrier function in aged skin. In addition to epidermal skin function, dermal function was also affected by collagen hydrolysate administration. In intrinsically aged skin, dermal ECM changes are accompanied by loss of skin elasticity. ECM in the dermis is a dense meshwork of collagen and elastin, embedded in a viscoelastic ground substance composed of proteoglycans and glycoproteins (69). In the collagen administered group, Mmp9 and Mmp13 (70) and Hpse (71), which function in ECM component degradation and tissue remodeling (72), were downregulated. Conversely, some glycoproteins contained in the ECM, such as Cspg4, Fn1, and Prg4 (69), were

upregulated. These results suggest that oral administration of collagen hydrolysate contributed to the inhibition of MMP-induced ECM breakdown and production of a number of ECM components resulting in maintenance of dermal elasticity.

I consider that the key factor of these effects may be Hyp-containing peptides in the collagen hydrolysate. By skin aging, collagen synthesis is decreased (73). Hyp facilitates the synthesis of collagen in the skin, and collagen hydrolysate contains a high concentration of Hyp and Hyp-containing peptides (16). Previous study also reports that not only amino acids, but also collagen-derived peptides such as Pro-Hyp, Ala-Hyp, and Gly-Pro-Hyp, were detected in human blood after oral intake of collagen hydrolysate (17). Shimizu *et al.* (74) demonstrated in an *in vivo* study that administration of a collagen-derived Pro-Hyp and Hyp-Gly improved an HR-AD diet intake-induced dry skin condition in the hairless mouse. These peptides ameliorated skin barrier dysfunction such as degradation of TEWL and epidermal water content and altered muscle related-genes expression.

In particular, cell proliferation and synthesis of HA, a glycosaminoglycan, were induced by the major dipeptide Pro-Hyp in human dermal fibroblasts (20). Furthermore, in chapter 1, I showed that collagen hydrolysate administration suppressed a decrease in dermal HA content induced by UVB in hairless mice. Thus, in the present study, bioactive components of collagen hydrolysate, such as Pro-Hyp, probably led to suppression of ECM degradation and facilitation of ECM component production in the dermis. Previous studies have shown that collagen-derived peptides can modulate the condition of dermal fibroblasts (19, 75). Whereas there are positive effects on Pro-Hyp induced epidermal cell production and differentiation in a coculture of keratinocytes with fibroblasts, however, it was not observed in keratinocytes alone (76). Based on the

data in this chapter, I hypothesize that collagen-derived peptides directly or indirectly affect all layers of the skin through the basement membrane. Because Pro-Hyp and Gly-Pro-Hyp are chemotactic and have the potential ability to aid wound repair (19, 75), these peptides may stimulate production of keratinocytes in the basal layer. Further studies are needed to clarify the mechanisms underlying the effects of such peptides on the epidermis in detail.

Consequently, this study show that long-term collagen hydrolysate administration improved epidermal barrier function and dermal elasticity of intrinsically aged skin as a result of a positive regulation of expression of genes related to production and maintenance of skin tissues. Continuous intake of dietary collagen hydrolysate is probably effective for preventing skin dysfunction by chronological aging such as age-induced dryness and sagging and is expected to be favorable for the homeostatic regulation of the skin.

Chapter 3:

A novel mechanism for improvement of dry skin by dietary milk phospholipids: Effect on epidermal covalently bound ceramides and skin inflammation in hairless mice

3-1 Introduction

It has been demonstrated that milk phospholipid concentrates increased the SC hydration and reduced TEWL in normal hairless mice (77). However, the mechanisms by which milk derived phospholipids improve skin barrier functions have yet to be elucidated. Sphingomyelin (SM) is not only a constituent of cell membranes, but also a dietary component. SM is abundant in eggs, meat, milk, and fish (78-80). Supplementation with SM has been reported to have beneficial effects on disease prevention and health maintenance, such as lowering serum cholesterol (81), preventing colon cancer (82, 83), improvement of skin barrier function (84).

Reduced barrier function appears to be a consequence of inadequate structural conditions in the epidermis. The SC has primarily skin barrier properties, which is the outermost layer of the epidermis. The SC consists of corneocytes surrounded by an intracellular matrix that is enriched in neutral lipids. Ceramides, which comprise approximately 50 wt% of intercellular lipids in the SC, have an important role in retaining epidermal water and, in combination with cholesterol and free fatty acids, influence the epidermal barrier permeability. In bovine milk, phospholipids represent approximately 0.5% to 1% of the total lipid content, and mainly consist of SM and phosphatidylcholine. Haruta-Ono *et al.* reported that orally administrated SM

incorporated into skin SM and converted to SC ceramide (84) and other study showed that sphingoid base, sphingosine, improves transepithelial electric resistance value in SDS treated-keratinocytes (85). However, the mechanisms by which milk SM improve skin barrier functions remain unclear.

Recent research in NC/Nga mice demonstrated that dietary sericin (86) or gromwell (87) improved epidermal skin dryness due to increased levels of non-protein bound glucosylceramides and ceramides and up-regulation of glucosylceramide synthase, β-glucocerebrosidase, and acidic sphingomyelinase. The epidermis also contains covalently-bound ω-hydroxy ceramides that are most frequently bound to a structural protein in the epidermal CE by an ester linkage. Levels of covalently-bound ω-hydroxy ceramides were shown to be significantly decreased after UVB irradiation, tape-stripping, or treatment with sodium dodecyl sulfate, whereas the levels of non-bound ceramides remained unchanged (88). Lipid species of this type are therefore thought to play a crucial role in the formation of lamellar structures, and are involved in the maintenance of the skin barrier function (89, 90).

Dry skin conditions, such as atopic dermatitis (AD) and psoriasis vulgaris, cause chronic skin inflammation. Although the pathogenesis of dry skin conditions is not completely understood, it is thought to involve a Th2 cell-mediated allergic inflammatory cascade. Skin injury, caused by environmental allergens, scratching, or microbial toxins, activates keratinocytes to release proinflammatory cytokines and chemokines that induce the expression of adhesion molecules on the vascular endothelium and facilitate the extravasation of inflammatory cells into the skin (91). Serum levels of thymus and activation-regulated chemokine (TARC) (92), thymic stromal lymphopoietin (93), and soluble P-selectin (sP-selectin) (94) could be

significantly higher in patients with AD than in people without this type of skin condition. Thus, serum markers of chemokines and platelet activator appear to be useful for assessing the severity of dry skin conditions. However, few studies have been able to demonstrate that the oral intake of dietary components can modulate both reduction of covalently-bound ω-hydroxy ceramides and skin inflammation associated with skin dryness. It is well known that feeding hairless mice a magnesium-deficient HR-AD diet for an extended period of time causes a skin barrier defect characterized by an increase in TEWL and a decrease in skin hydration (95-98). Fujii *et al.* have previously reported that hairless mice fed the HR-AD diet develop skin inflammation accompanied by a skin barrier defect and itch-related scratching (96, 98). This study was designed to examine the effect of dietary SM on covalently-bound ω-hydroxy ceramides and skin inflammation markers in hairless mice fed the HR-AD diet with the aim of elucidating a novel mechanism by which SM may improve skin barrier function.

3-2 Methods

Animals

Four-weeks-old female Hos:HR-1 hairless mice (Japan SLC Inc., Shizuoka, Japan) were used in this experiment. Same as described in chapter 1-2, all mice were housed individually in plastic cages in a temperature- and humidity-controlled room and maintained on a 12 h light-dark cycle. All of the animal experiments in this study were approved by Meiji Co., Ltd. Institutional Animal Care and Use Committee, and performed in accordance with the Guiding Principles for the Care and Use of Laboratory Animals approved by Meiji Co., Ltd.

Skin evaluation in a dry skin mouse model

After acclimatization for 7 days, forty mice were randomized into one of four groups (n=10/group), and fed either a standard (control) diet (F-2; Funabashi Farm, Chiba, Japan), the HR-AD diet (Norsan Corp., Kanagawa, Japan), or the HR-AD diet supplemented with either 7.0 g/kg (low [L]-SM) or 41.0 g/kg (high [H]-SM) of milk phospholipids (MPLs) (Phospholipid concentrate 700, Fonterra Co-operative Group Ltd., New Zealand). Mice were allowed free access to food and water *ad libitum*. The MPLs consisted of 16.0% SM, 31.0% phosphatidylcholine, 3.0% phosphatidylserine, and 8.7% phosphatidylethanolamine. The remaining components included 25.8% other lipids, 2.5% moisture, 6.5% lactose, and 6.0% minerals. The magnesium content in the experimental diets was 200 mg/g (control), 17.6 mg/g (HR-AD), 17.5 mg/g (L-SM), and 17.2 mg/g (H-SM).

The water content of the SC and TEWL was measured at baseline (time 0) and after 2, 4, 6, and 8 weeks of feeding. After 8 weeks of feeding, all mice were euthanized under isoflurane anesthesia. Blood samples were collected and subsequently centrifuged at 1,000 g at 4^{o}C; serum samples were stored at -80^{o}C until analysis. Skin was quickly excised and immediately frozen at -80^{o}C until the time of assay.

The TEWL and water content of the SC were assessed under standardized conditions as described in chapter 1-2. Both parameters were measured with and a Corneometer® (Courage and Khazaka Electronic GmbH, Cologne, Germany), a Tewemeter MPA580 (Courage and Khazaka Electronic GmbH, Cologne, Germany), respectively. For histological analysis and measurement of epidermal thickness, dorsal skin sections were stained with H&E. The thickness of the epidermis was measured as described in chapter 1-2.

Analysis of covalently-bound ω-hydroxy ceramides

Covalently-bound ceramides was extracted using a modification of the method reported by Macheleidt *et al.* (99). Epidermal sheets were obtained from dosal skin samples by treating them with Dispase®II (Roche, IND, USA) at 4°C overnight. Tissues were homogenized in chloroform/methanol (2 : 1, v/v) using a glass homogenizer. After removal of the supernatant by centrifugation, a chloroform/methanol solution was added to wash the protein residue twice. After drying, protein pellets were incubated in 1 M KOH in 95% methanol at room temperature overnight to release the lipids covalently-bound to the SC by ester-like bonds. The methanolic layer was removed after centrifugation and neutralized with 1 N HCl. The protein pellets were washed using chloroform/methanol (2 : 1, v/v). The organic phases were combined, dried, and redissolved in methanol. The protein pellet was immersed into 0.1 M sodium hydroxide solution containing 1% sodium dodecyl sulfate and incubated at 60°C for 2 hr to solubilize the protein. After incubation, the solution was neutralized with 1 N HCl. The protein concentration was assayed using a commercial kit (Micro BCA assay kit, Pierce Biotechnology, Inc., IL, USA). Covalently-bound ceramides in the mice epidermis were identified using a high performance liquid chromatography system coupled to a tandem mass spectrometer (HPLC-MS/MS) (Quattro premier XE, Waters Corporation, Milford, MA, USA). All the analyses were performed on a 2 X 100 mm column with a particle size of 1.7 μm (ACQUITY UPLC® BEH C18, Waters Corporation). Mobile phase A consisted of 5 mM ammonium acetate in 95% methanol, whereas mobile phase B consisted of 5 mM ammonium acetate in acetonitrile. The initial eluent composition was 100% A, followed by an increase to 100% B for 30 min, 100% B for 2 min, and then a reduction to 0% A for 3 min. Total running time was 35 min. The eluent flow was 0.4

mL/min and the column temperature was set at 40°C. Analytes were detected using electrospray ionization in the positive mode. Multiple-reaction-monitoring (MRM) was performed using characteristic fragmentation ions (*m/z* 750.7/264.3 for d18:1-C30:0, *m/z* 778.8/264.3 for d18:1-C32:0, *m/z* 776.8/264.3 for d18:1-C32:1, *m/z* 806.8/264.3 for d18:1-C34:0, *m/z* 804.8/264.3 for d18:1-C34:1, *m/z* 832.8/264.3 for d18:1-C36:1, *m/z* 764.8/250.2 for d17:1-C32:0, *m/z* 762.8/250.2 for d17:1-C32:1, *m/z* 790.8/250.3 for d17:1-C34:1, *m/z* 818.8/250.2 for d17:1-C36:1). The parameters for HPLC-MS/MS analysis were as follows: capillary voltage 3000 V, source temperature 120°C, desolvation temperature 400°C, desolvation gas flow 850 L/hr, cone gas flow 50 L/hr, cone voltage 40 V, and collision energy 30 eV.

Skin gene expression and serum inflammation makers analysis

Total RNA was isolated from dosal skin samples and synthesized cDNA as described in chapter 2-2. Real-time PCR was performed using the ABI 7500 Fast Realtime PCR systems. Primers and probes (TaqMan® Gene Expression Assays) were designed at Applied Biosystems from gene sequences obtained from GenBank (TSLP: Mm01157588_m1, TARC: Mm01244826_g1, β-actin [internal control]: Mm00607939_s1). Data were analyzed by 7500 software using $2^{-\Delta\Delta Ct}$ methods (100) and the results expressed as arbitrary units.

Serum total immunoglobulin E (IgE) concentrations were analyzed using an enzyme-linked immunosorbent assay (ELISA) kit (Shibayagi, Gunma, Japan). Serum TRAC, TSLP, sP-selectin were determined using an ELISA kit (R&D systems, MN, USA).

Statistical analysis

All data are presented as means ± SE. Data were subjected to one-way ANOVA with

post hoc analyses being carried out using Tukey's honestly significant difference test (SPSS ver.22.0, SPSS, IL, USA). The correlation between ω-hydroxy ceramide content and both TEWL and water content of the SC was calculated. Associations between the variables were examined using Pearson's correlation coefficient. Differences among groups were considered to be significant at $P < 0.05$.

3-3 Results

The water content of the SC and TEWL

A significant decrease in the water content of the SC was observed in the HR-AD group, as compared with the control group at 2, 4, 6, and 8 weeks. Supplementation with MPLs containing SM to the HR-AD diet significantly increased the water content of the SC at 4, 6, and 8 weeks. Skin hydration was significantly higher in the H-SM group than in the L-SM group at 6 and 8 weeks. The water content of the SC was not different between the control group and the H-SM group at 2 and 8 weeks (Fig 10a). TEWL was significantly increased in the HR-AD group compared with the control group at 4, 6, and 8 weeks. The addition of SM as MPLs to the HR-AD diet significantly suppressed an increase in TEWL at 4, 6, and 8 weeks. TEWL were significantly lower in the H-SM group than in the L-SM group at 6 and 8 weeks. TEWL was not different between the control group and H-SM group at every time point assessed (Fig 10b).

Appearance of mice, histology and epidermal thickness

On the overall appearance, supplementation with SM improved the skin condition in a dose-dependent manner (Fig 11). Mice fed the HR-AD diet, were observed layered parakeratosis, hyperplasia, keratinocyte apoptosis, and inflammatory cell infiltration in

histological images (Fig 12). Epidermal thickness was lower in mice fed the control and the H-SM diet compared with those fed the L-SM and the HR-AD diet in Fig 13.

Covalently-bound ω-hydroxy ceramides in the epidermis

A typical chromatogram of covalently-bound ω-hydroxy ceramides in the epidermis of hairless mice obtained is shown in Fig 14a using HPLC-MS/MS. Based on recent research that identified sphingolipids containing three molecular species of sphingoid bases, which were located in the epidermis of hairless mice (specifically d17:1, d18:1, and d18:0) (101), a qualitative analysis of covalently-bound ω-hydroxy ceramides targeting these molecular species of sphingoid bases using HPLC-MS/MS were performed. From the epidermis of hairless mice, eleven molecular species of protein-bound ω-hydroxy ceramides which consisted of d18:1-C30:0, d18:1-C32:0, d18:1-C32:1, d18:1-C34:0, d18:1-C34:1, d18:1-C36:1, d17:1-C32:0, d17:1-C32:1, d17:1-C34:0, d17:1-C34:1, and d17:1-C36:1 were identified. The peak intensity of ω-hydroxy tetratriacontenoic-sphingosine (d18:1-C34:1) was highest in the epidermis. The data for covalently-bound ω-hydroxy ceramide percentages in the epidermis are summarized in Table 6. The HR-AD diet significantly decreased all ω-hydroxy ceramide molecular species compared with the control diet. The levels of ω-hydroxy ceramides in d18:1-C32:1 and d18:1-C34:1 were significantly increased in both the H-SM and the L-SM groups compared with the HR-AD group, while the levels of other ω-hydroxy ceramides were significantly increased in the H-SM group only compared with the HR-AD group. The ω-hydroxy ceramides levels linked to very long-chain fatty acids in d18:1-C36:1 and d17:1-C36:1 were not different between the control and the H-SM group. Fig 14b shows the correlation between ω-hydroxy ceramide contents and both TEWL and the SC water content. A significant and strong correlation was observed

between the covalently-bound ω-hydroxy ceramide d18:1-C34:1 and skin hydration (r = 0.87, $P < 0.001$) and the covalently-bound ω-hydroxy ceramide d18:1-C34:1 and TEWL (r = -0.91, $P < 0.001$).

Skin chemokine mRNA levels

Significantly higher levels of mRNA for both TSLP and TARC were observed in the HR-AD group compared with the control group (Fig 15). The level of TSLP mRNA was significantly lower in the H-SM group only, whereas the level of TARC mRNA was significantly lower in both the L-SM and the H-SM groups compared with the HR-AD group. eFurthermore, the levels of both TSLP and TARC mRNA were low in mice fed the control and the H-SM diet compared with those fed the L-SM and HR-AD diet.

Serum parameters

Serum concentrations of IgE, TARC, TSLP, and sP-selectin were significantly higher in the HR-AD group than the control group (Fig 16). Compared with the HR-AD group, mice fed the L-SM or H-SM diet had significantly lower serum concentrations of IgE, TSLP, and sP-selectin; in addition, the H-SM-fed mice also had significantly lower serum concentrations of TARC. Moreover, the H-SM diet resulted in lower serum IgE, TARC, TSLP, and sP-selectin concentrations that were not different from the control mice.

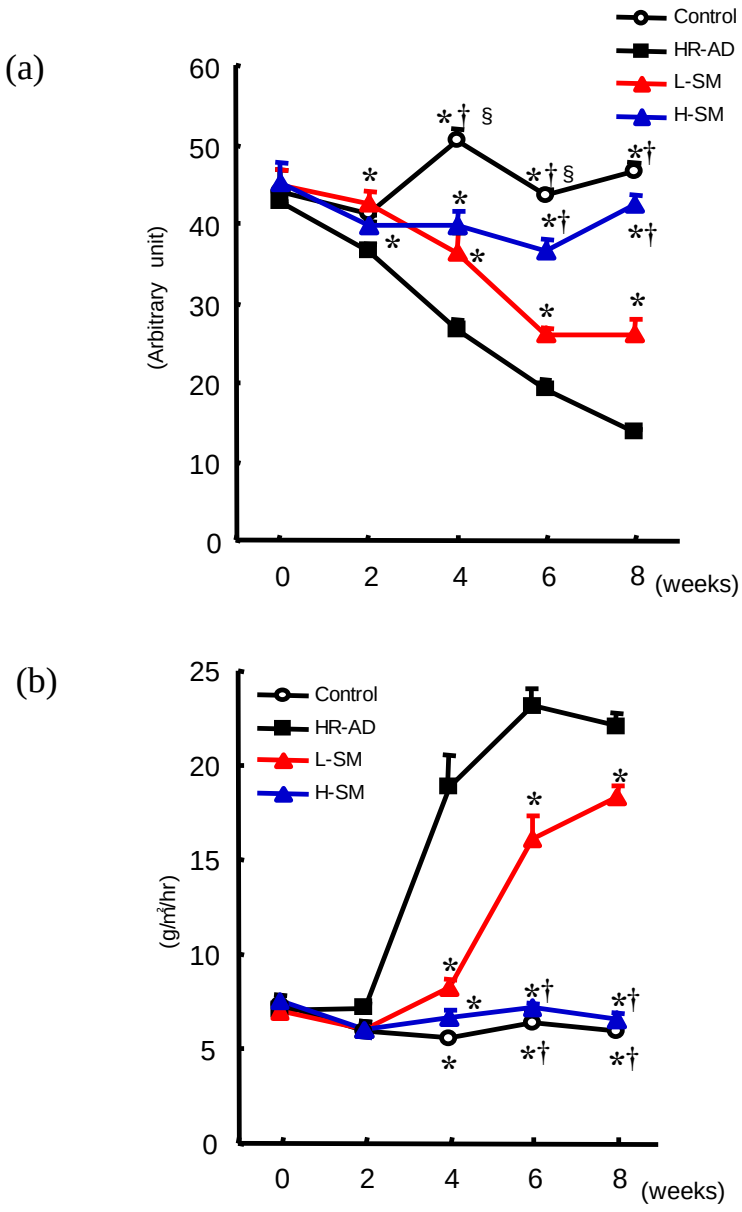

Fig. 10. Effect of dietary SM containing MPLs on changes the water content of the SC (a) and TEWL (b).

The values are means ± SE (n = 10). *P < 0.05 (vs. the HR-AD group), † P < 0.05 (vs. the L-SM group), §P < 0.05 (vs. the H-SM group).

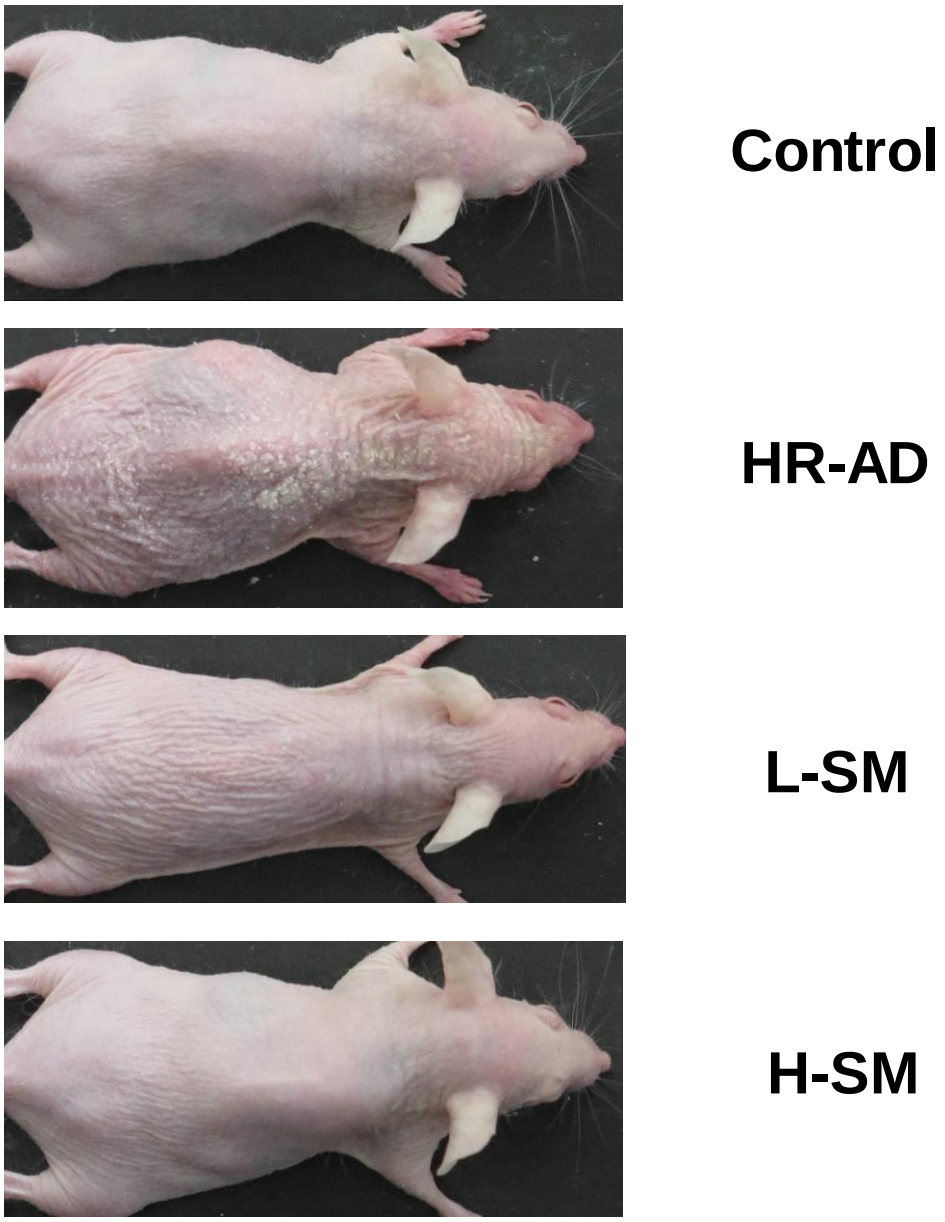

Fig. 11. Effect of dietary SM containing MPLs on the overall skin appearance of mice.

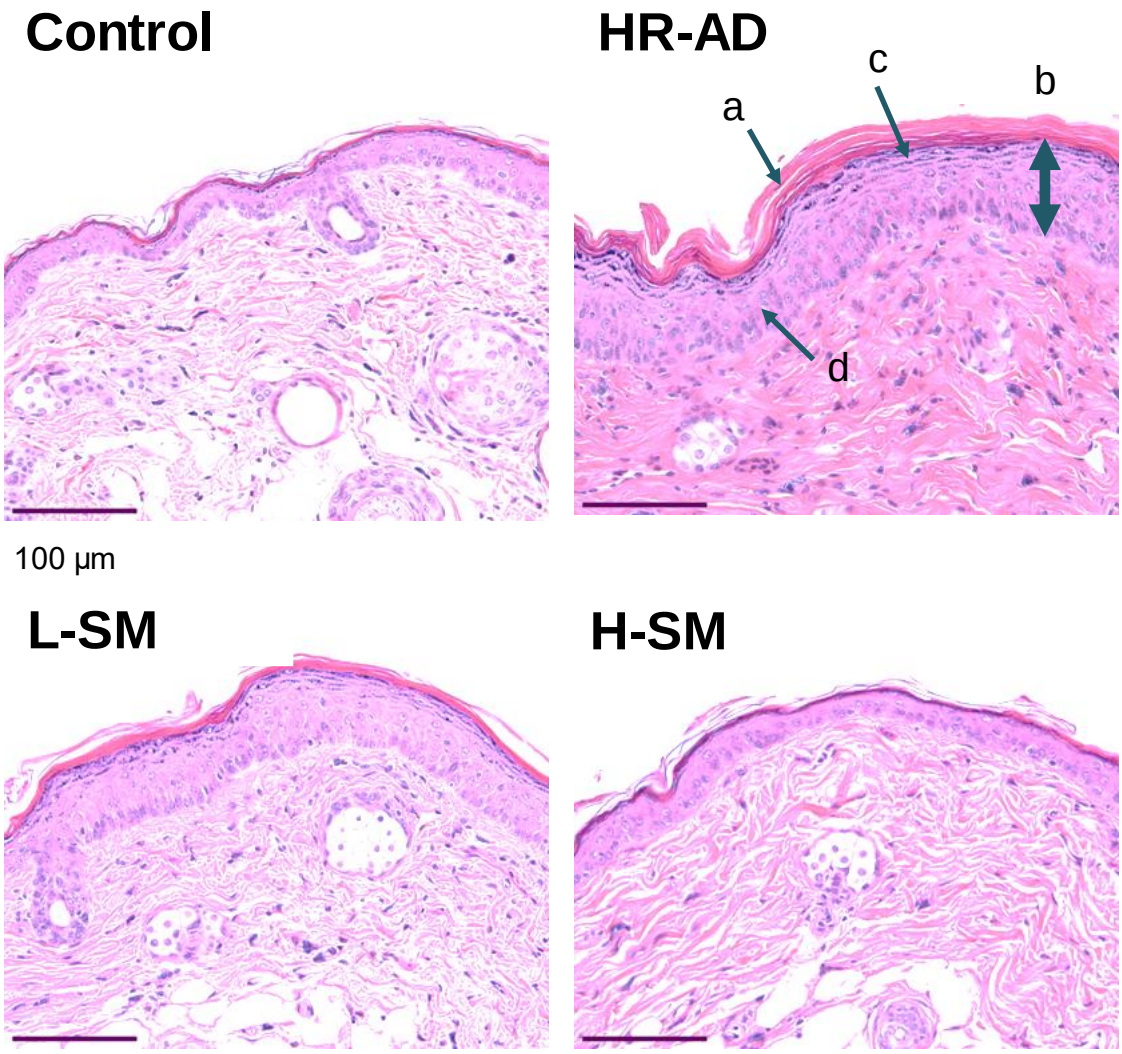

Fig. 12. Effect of dietary SM containing MPLs on skin histological images of mice.

Arrow head shows layered parakeratosis (a), hyperplasia (b), keratinocyte apoptosis (c), and inflammatory cell infiltration (d).

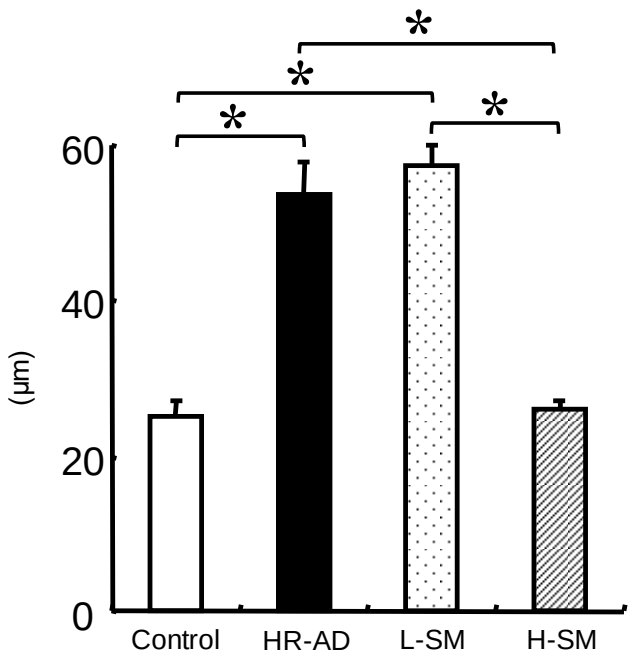

Fig. 13. Effect of dietary SM containing MPLs on epidermal thickness.

The values are means ± SE (n = 10). *$P < 0.05$ (between groups)

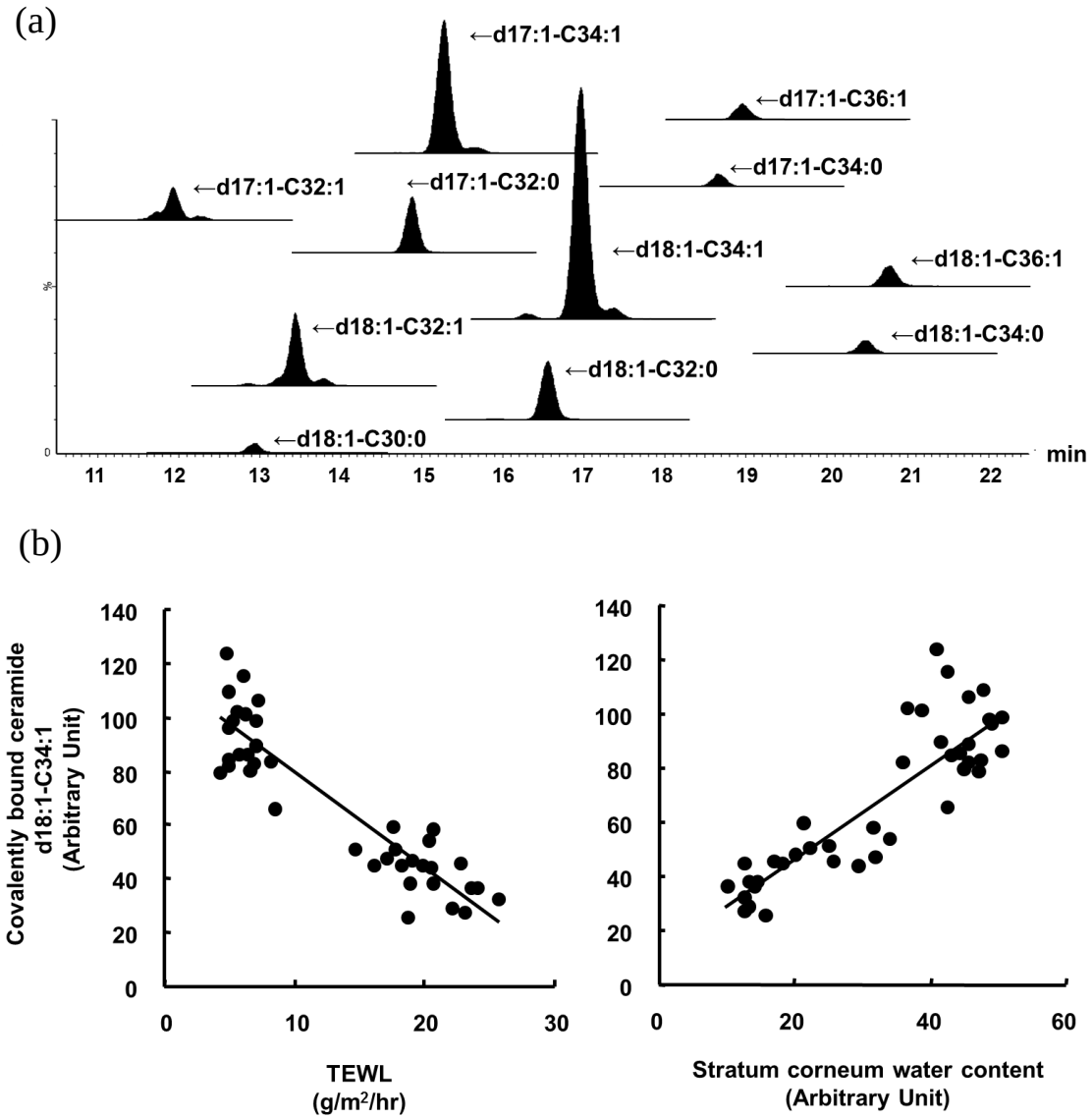

Fig. 14. Typical chromatogram of covalently-bound ω-hydroxy ceramides in the epidermis of hairless mice fed the normal diet using HPLC-MS/MS (a). Correlation between covalently-bound ω-hydroxy ceramide levels and both TEWL and the water content of the SC (b).

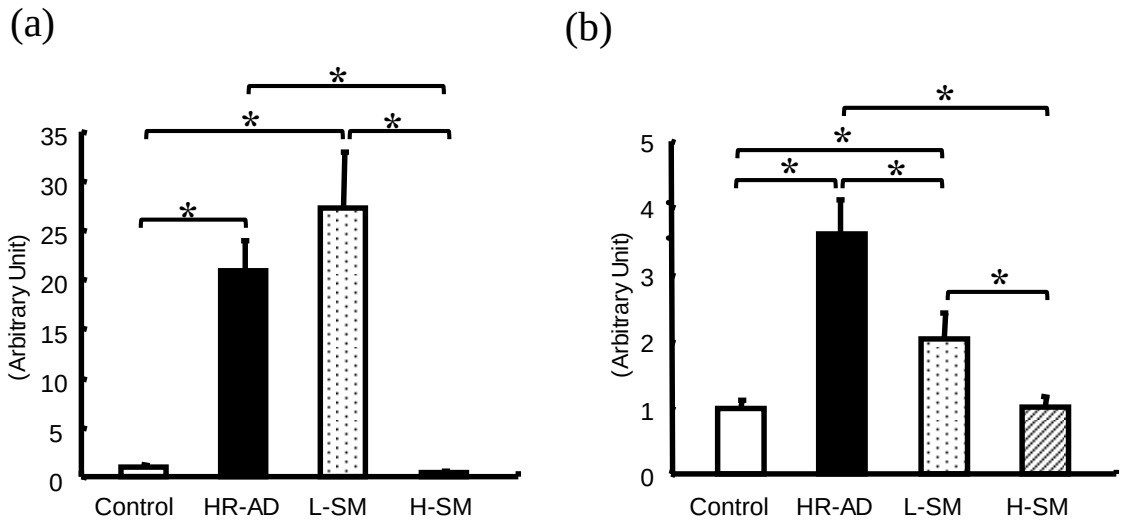

Fig. 15. Effect of dietary SM containing MPLs on chemokines, thymic stromal lymphopoietin (TSLP) (a), and thymus and activation-regulated chemokine (TARC) (b), and levels of mRNA in the skin.

The values are means ± SE (n = 10). *$P < 0.05$ (between groups)

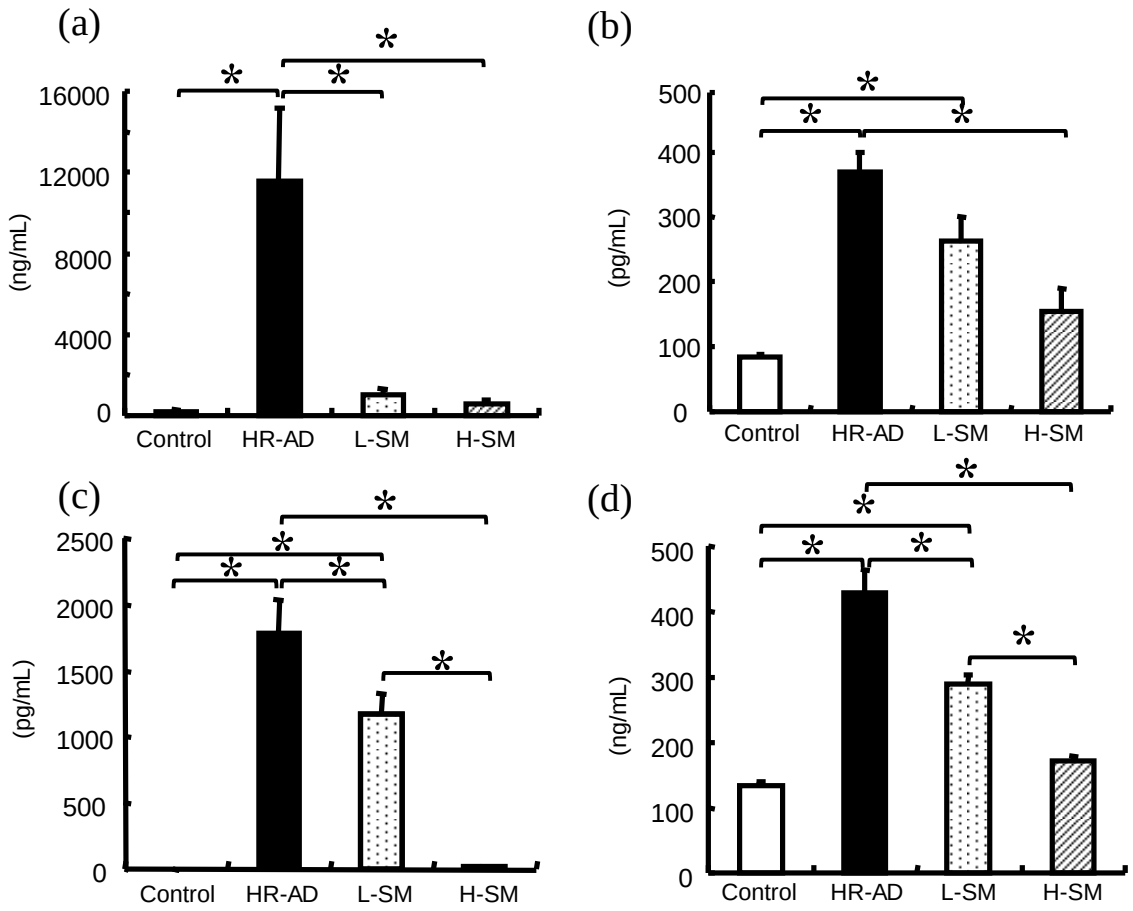

Fig. 16. Effect of dietary SM containing MPLs on serum immunoglobulin E (IgE) (a), thymus and activation-regulated chemokine (TARC) (b), thymic stromal lymphopoietin (TSLP) (c), and soluble P –selectin (sP-selectin) levels (d).

The values are means ± SE (n = 10). **P* < 0.05 (between groups).

Table 6. Effect of dietary SM containing MPLs on the percentages of covalently-bound ω-hydroxy ceramides in the epidermis of mice.

	Diet			
	Control	HR-AD	L-SM	H-SM
d18:1 – C30:0	100.0 ±14.4 *† §	8.3 ±0.8	14.2 ±1.2	43.4 ±3.6 *†
d18:1 – C32:0	100.0 ±7.9 *† §	11.4 ±1.0	16.6 ±1.1	59.1 ±4.7 *†
d18:1 – C32:1	100.0 ±4.7 *† §	28.3 ±2.0	45.0 ±1.5 *	63.7 ±2.9 *†
d18:1 – C34:0	100.0 ±11.5 *† §	9.1 ±0.9	11.8 ±1.0	66.3 ±6.5 *†
d18:1 – C34:1	100.0 ±4.2 *† §	34.9 ±2.2	49.8 ±1.7 *	84.8 ±3.3 *†
d18:1 – C36:1	100.0 ±6.8 *†	24.6 ±1.8	33.1 ±1.8	97.3 ±5.4 *†
d17:1 – C32:0	100.0 ±7.1 *† §	3.9 ±0.4	5.6 ±0.5	50.0 ±4.4 *†
d17:1 – C32:1	100.0 ±5.2 *† §	14.3 ±1.1	22.0 ±1.7	69.1 ±3.2 *†
d17:1 – C34:0	100.0 ±8.5 *† §	3.5 ±0.4	4.2 ±0.5	59.6 ±5.9 *†
d17:1 – C34:1	100.0 ±4.0 *† §	17.7 ±1.2	24.1 ±1.6	83.7 ±3.9 *†
d17:1 – C36:1	100.0 ±6.2 *†	12.2 ±1.1	15.9 ±1.4	95.7 ±6.6 *†

Data expressed as relative peak area per epidermal protein content.

The values are means ± SEM (n = 10/group).

*P < 0.05 (vs. the HR-AD group). † P < 0.05 (vs. the L-SM group). §P < 0.05 (vs. the H-SM group).

3-4 Discussion

This study showed that oral administration of MPLs improved dry skin conditions in hairless mice fed the HR-AD diet. Interestingly, MPLs containing SM attenuated a decrease in epidermal covalently-bound ω-hydroxy ceramide levels and an increase in inflammation marker levels in both serum and skin. Thus, MPLs attenuated dry skin conditions by modulating epidermal covalently-bound ω-hydroxy ceramides that are associated with formation of lamellar structures and skin inflammation in hairless mice fed the HR-AD diet.

It is well known that long-term feeding of the HR-AD diet to hairless mice causes a skin barrier defect characterized by an increase in TEWL and a decrease in skin hydration (95-98). However, it remains unclear whether reduced barrier function causes a consequential inadequacy of the structural condition of the epidermis. In this chapter, I focused on epidermal covalently-bound ω-hydroxy ceramides, which are thought to play a most crucial role in the formation of lamellar structures, resulting in retention of epidermal water and in the epidermal barrier (89, 90). A previous report showed that the amount of protein-bound ω-hydroxy ceramides in healthy epidermises comprised 46% to 53% of the total protein-bound lipids, whereas this amount was 10% to 25% lower in human subjects with affected atopic skin areas (99). In this experiment, the covalently-bound ω-hydroxy ceramides from murine epidermises were identified using HPLC-MS/MS. Eleven species of covalently-bound long-chain (C30-36) ω-hydroxy ceramides containing either C18:1 or C17:1 sphingoid base were identified in mice epidermises. The result showed the HR-AD diet was significantly associated with a lower level of all molecular species of covalently-bound ω-hydroxy ceramides in the epidermis of mice. A significant and strong correlation was observed between

covalently-bound ω-hydroxy ceramide (d18:1-C34:1) and skin hydration, as well as covalently-bound ω-hydroxy ceramide (d18:1-C34:1) and TEWL (Fig 14b). Thus, one possible explanation for the observed dysfunction in the skin barrier may be associated with the reduction in covalently-bound ceramides in the epidermis. Considering that ceramides in the SC comprise more than 350 molecular species, it is important to confirm that those specific molecular species of ω-hydroxy ceramides are implicated in skin barrier function (102). A recent clinical study showed that the smaller species of ceramides (< 40 total carbons) were expressed at significantly higher levels and the larger species (> 50 total carbons) were expressed at significantly lower levels in patients with AD sites versus healthy subjects (103). In addition, it is well known that the ratio of unsaturated and saturated fatty acids in phospholipids influences membrane fluidity. Bouwstra *et al.* (104) demonstrated that the degree of saturation of the fatty acid chain of ceramide-1 had marked effects on lamellar and lateral lipid organization *in vitro*. The long periodicity phase was present predominantly in mixtures prepared with ceramide-1 linoleate, and absent in mixtures prepared with ceramide-1 stearate. This study demonstrated that the HR-AD diet fed mice had notably reduced mean percentages of covalently-bound ω-hydroxy ceramides with saturated fatty acids (C30:0, C32:0, and C34:0) ranging from 3.5% to 11.4%, whereas ceramides with unsaturated fatty acids (C32:1, C34:1, and C36:1) ranged from 14.3% to 34.9% (Table 6). I consider that it is likely that the difference in carbon chain length and the ratio of unsaturated fatty acids to saturated fatty acids of ω-hydroxy ceramides is also associated with skin barrier structure, although the manner by which such effects may be exerted is not fully understood.

This study provides evidence that the oral intake of MPLs improved the skin barrier

function in mice fed the HR-AD diet. MPLs contains 16% of SM, which consists of three main components; a phosphocholine head group, a sphingoid base, and a fatty acid. Several studies have reported that dietary sphingolipids, such as SM and glucosylceramide, improve skin barrier function. Orally-administered milk SM was implicated in the water holding capacity of skin in hairless mice (84). SM from porcine brain was used to accelerate the recoveries of damaged skin caused by skin barrier function impairments in both HR-AD-fed and tape-stripped injured mouse models (95). Dietary glucosylceramide was also shown to improve the recovery of SC flexibility and reduce TEWL in acutely barrier-perturbed mice (95, 105). Dietary sphingolipids are hydrolyzed by intestinal enzymes to their components, sphingoid bases, fatty acids, and the polar head group and then taken up into mucosal cells (106-109). Therefore, ingestion of sphingolipids which structurally consist of sphingoid bases may contribute to skin barrier function.

SM caused significant increases in the percentage of covalently-bound ω-hydroxy ceramides in the epidermis. Results of a recent *in vitro* study using cultured keratinocytes showed that sphingadienine (d18:2) enhanced CE formation via expression of transglutaminase-1 (TGase-1), and played a potential role in the covalent bonding of ω-hydroxy ceramides to peptide moieties in the outer CE (110). This study showed that the HR-AD diet led to significant increases in mRNA level of TGase-1, while SM attenuated the increase in this gene expression in a dose-dependent manner (data not shown). The decrease in TGase-1 mRNA level despite an increase in covalently-bound ω-hydroxy ceramides is presumably due to negative feedback regulation. Furthermore, milk SM consists mainly of sphingosine (d18:1), but not sphingadienine (d18:2) (111). As a consequence, it is possible that factors other than

TGase-1 may regulate the production of covalently-bound ω-hydroxy ceramides in mice fed MPLs. However, further studies are needed to clarify this mechanism.

Dry skin conditions, such as AD and psoriasis vulgaris cause chronic skin inflammation. This study provided evidence that levels of TSLP and TARC mRNA, and serum concentrations of IgE, TARC, TSLP, and sP-selectin were significantly higher in the HR-AD group compared with the control group. The focus of this study was on changes in the levels of skin TSLP mRNA and serum concentration changes in TSLP, and these were 20-fold and 110-fold higher, respectively, in mice fed the HR-AD diet, representing a dramatic difference in comparison with mice fed the standard diet. Recent compelling evidence indicates that TSLP may have a determinant role in the initiation and maintenance of allergic immune responses (112, 113). TSLP modulates polarization of dendritic cells by increasing secretion of Th2 cell-attracting chemokines, such as TARC. TSLP was highly expressed by keratinocytes in AD lesions and its expression was associated with the migration and activation of Langerhans cells (114). Thus, TSLP might be a sensitive marker of dry skin conditions, and play a crucial role in the pathogenesis of such in hairless mice.

This study showed for the first time that SM added to the HR-AD diet fed to mice, attenuated inflammation parameters in both skin and serum. In particular, a high dose of SM versus a low dose is more effective at attenuating levels of TSLP in the skin and serum. Several potential mechanisms can be proposed to explain the beneficial effect SM can have on skin inflammation. One explanation may be related to the improvement in skin barrier function. Skin barrier dysfunction allows entry of allergens, antigens, and chemicals from the environment, which can activate keratinocytes to release pro-inflammatory cytokines and chemokines (91). It is therefore suggested that dietary

SM help to mitigate skin barrier dysfunction and protect against the entry of environmental agents, thereby attenuating skin inflammation in mice. Another possibility is that sphingolipids may be a source of anti-inflammatory properties. Sphingosine is a potent inhibitor of protein kinase C activity *in vitro* (115). Treatment with sphingosines inhibited phorbol ester-induced skin inflammation via inactivation of protein kinase C in mice (116). In addition, the oral administration of sphingolipids significantly downregulated the activation of TNF-α at an inflammatory site (117). Although it remains unclear whether oral intake of sphingolipids directly inhibits skin inflammation, future studies are needed to clarify the potential underlying mechanism.

In conclusion, dietary SM improved dry skin conditions in hairless mice fed the HR-AD diet. Furthermore, adding SM attenuated the decrease in epidermal protein-bound ω-hydroxy ceramide levels associated with the intake of the HR-AD diet, and was associated with a lower level of skin and serum markers of inflammation. SM, might increase the strength of epidermal lamellar structures and suppress skin inflammation, to thereby improve skin barrier functions. However, since MPLs, used as a source of SM in this experiment, also contain several phospholipids and components other than SM, the effect of their contents should be considered and effect of SM on the skin also should be demonstrated in other experimental models. Moreover, a limitation of this study was that the pathogenic mechanism of dry skin induced by a nutritionally-deficient diet (HR-AD) is different from that induced by epicutaneous sensitization or genetic modification (118, 119). Further studies are therefore needed to elucidate the beneficial effect of SM on dry skin condition using other animal models that have similarities to this condition in humans.

Chapter 4:

Dietary milk sphingomyelin prevents disruption of skin barrier function in hairless mice after UVB irradiation

4-1 Introduction

A single UVB irradiation dose has long been known to cause skin barrier dysfunction as well as increased TEWL and decreases in the water content of the SC. UVB irradiation of mammalian skin disrupts epidermal permeability barrier functions, and is accompanied by an increase in TEWL (3, 5, 120) as well as alterations in the SC lipid profile (121, 122). Previous studies showed that levels of covalently-bound ceramides, but not unbound-ceramides, were significantly reduced in parallel with a marked increase in TEWL following irradiation with a single UVB dose in hairless rodents (88, 122). Furthermore, the CE is formed during terminal differentiation of the epidermis through crosslinking of specific precursor proteins, including involucrin, loricrin, small proline-rich proteins, and transglutaminase (TGase), which are essential for skin barrier function (90, 123). Therefore, lipid species such as ω-hydroxy ceramides, together with CE components are thought to play a crucial role in the formation of lamella structures, and are involved in maintaining skin barrier functions. However, few studies have been able to demonstrate that the oral intake of dietary components can modulate epidermal structures associated with dryness induced by UVB irradiation. Therefore, in present study I evaluated the effects of dietary milk derived-SM on skin barrier defects induced by a single dose of UVB irradiation in hairless mice.

4-2 Methods

Animals

Sixty-four nine-weeks-old female hairless mice (Hos: HR-1, Nippon SLC Inc., Shizuoka, Japan) were used in this experiment. All mice were housed in plastic cages (four mice/cage) in a temperature- and humidity-controlled room (24 ± 1 °C and 50 ± 10% relative humidity [RH]) under a 12 hour light-dark cycle. Mice were allowed free access to the standard diet AIN-93G (Oriental Yeast Co., Ltd., Tokyo, Japan) and water. The animal experiments in this chapter were approved by Meiji Co., Ltd. Institutional Animal Care and Use Committee, and performed in accordance with the Guiding Principles for the Care and Use of Laboratory Animals approved by Meiji Co., Ltd (Permit Number: 2013_3871_0082). All surgery was performed under isoflurane anesthesia, and all efforts were made to minimize suffering.

Experimental design

After acclimatization for 4 days, mice were randomized into 8 groups (control groups [day 0, 1, 2, 3] and SM groups [day 0, 1, 2, 3]), according to body weight, SC water content, and TEWL. The control group was given 5% ethanol solution at 10 mL/kg body weight, while the other groups were given SM at 146 mg/5% ethanol solution at 10 mL/kg body weight. SM from milk (certified ≥ 98% purity, NS220204) was purchased from Nagara Science Co., Ltd. (Gifu, Japan). Mice were given the experimental SM samples orally for 10 days, from 7 days before UVB irradiation (day -7) until 3 days after irradiation (day 3). Seven days after the initiation of the experimental sample administration (day 0), the dorsal skin was exposed once to 20 mJ/cm^2 emitted by a UVB lamp under isoflurane anesthesia as another experiment of UVB irradiation in chapter 1-2. SC water content and TEWL were measured 7 days

before and 0, 1, 2, and 3 days after irradiation. All mice were euthanized under isoflurane anesthesia on day 0, 1, 2, or 3. The dorsal skin was excised quickly and immediately frozen at -80 °C until analysis.

Measurement of SC water content and TEWL

SC water content and TEWL were assessed under standardized conditions as described in chapter 1-2.

Quantitative measurement of gene expression

Dorsal skin samples from each mouse were frozen in liquid N_2 and powdered. Total RNA was isolated from the skin samples in accordance with guanidine thiocyanate method (124) using TRIzol reagent (Life Technologies Corporation, Carlsbad, CA, USA), and purified with an RNeasy Mini Kit (Qiagen, Hilden, Germany). Extracted RNA was dissolved in diethylpyrocarbonate-treated water and quantified spectrophotometrically at a wavelength of 260 nm. Reverse transcription was performed using a RivertAid First Strand cDNA Synthesis Kit (Thermo Fisher Scientific, Waltham, MA, USA). The cDNA was stored at -80 °C prior to subsequent analysis. Quantitative real-time reverse transcription polymerase chain reaction (RT–PCR) analysis was performed using the ABI 7500 Fast Realtime PCR system (Applied Biosystems, Foster City, CA, USA). The respective primers and probes (TaqMan Gene Expression Assays) were designed at Applied Biosystems from gene sequences obtained from GenBank (thymic stromal lymphopoietin [TSLP]: Mm01157588_m1, IL-1 beta: Mm00434228_m1, IL-6: Mm00498375_m1, loricrin: Mm01962650_s1, TGase-3: Mm00436999_m1, glyceraldehyde-3-phosphate dehydrogenase [GAPDH]: Mm99999915_g1). The relative expression of the gene of interest was normalized relative to GAPDH mRNA levels and then calculated using the $2^{-\Delta\Delta Ct}$ method (125).

The results are expressed as arbitrary units.

Analysis of covalently-bound ceramide content by HPLC/MS/MS

Extraction and identification of covalently-bound ceramides in mouse epidermal tissues were performed as described in chapter 3-2. Molecular species of ceramide, ω-hydroxy tetratriacontenoic-sphingosine (d18:1-C34:1), was the main component in the epidermis. Data are expressed as the relative peak area per epidermal protein content.

Statistical analysis

All data are presented as means ± SD. The RT-PCR results were expressed as fold change ± SD. Data were analyzed by two-way ANOVA with post hoc analyses being carried out using Dunnett's test (time) and Student's t-test (group) (SPSS ver. 22.0, SPSS, IL, USA). The statistical analyses of gene expression were performed at the ΔCt stage in order to exclude potential bias due to the averaging of data transformed through the equation $2^{-\Delta\Delta Ct}$ (53). Differences among groups were considered to be significant at $P < 0.05$.

4-3 Results

A single dose of UVB irradiation significantly decreased the SC water content (Fig. 17a) and increased TEWL (Fig. 17b) at every time point assessed. The water content of SC was significantly higher in the SM group than the control group on days 2 and 3. Meanwhile, TEWL was significantly lowered in the SM group relative to the control group on days 2 and 3 after irradiation. Levels of ω-hydroxy tetratriacontenoic sphingoshine (d18:1-ω-hydroxy C34:1) in the epidermis are shown in Fig. 18. On 3 days after UVB irradiation, the level of covalently-bound ω-hydroxy ceramide was

significantly decreased in both groups. However, covalently-bound ω-hydroxy ceramide content was significantly lower in the control group relative to the SM group.

A significant up-regulation of skin inflammation-related genes, TSLP, IL-1 beta, and IL-6 mRNA levels, was observed in the control group on day 1 and 2, while TSLP and IL-6 mRNA levels were significantly increased in the SM group at every time point assessed (Fig. 19). After UVB irradiation, there was no change in the levels of IL-1 beta mRNA in the SM group. The mRNA level of TSLP was significantly higher in the control group than the SM group on day 0 and 1, while the mRNA level of IL-1 beta on day 1 and 2 was markedly increased for the control group and relatively constant for the SM group (Figs. 19a, b). Meanwhile, IL-6 levels increased in the control group on day 1 after UVB irradiation before tapering on days 2 and 3, while the SM group showed a similar expression pattern but with lower levels of mRNA (Fig. 19c). Loricrin and TGase-3 are known as enhancement factors of epidermal CE structures in the epidermis. The mRNA levels of loricrin exhibited a significant decrease in the control group on day 1 and 2 after UVB irradiation, while for the SM group loricrin mRNA levels were maintained until day 2 (Fig. 20a). The mRNA level of loricrin was significantly higher in the SM group than in the control group on day 1 after UVB irradiation. The mRNA level of TGase-3 showed a significant increase in the control group on days 2 and 3, while for the SM group increased levels were observed on day 1 and particularly day 2 (Fig. 20b). The mRNA level of TGase-3 showed a significant higher in the SM group than in the control group on days 1 and 2.

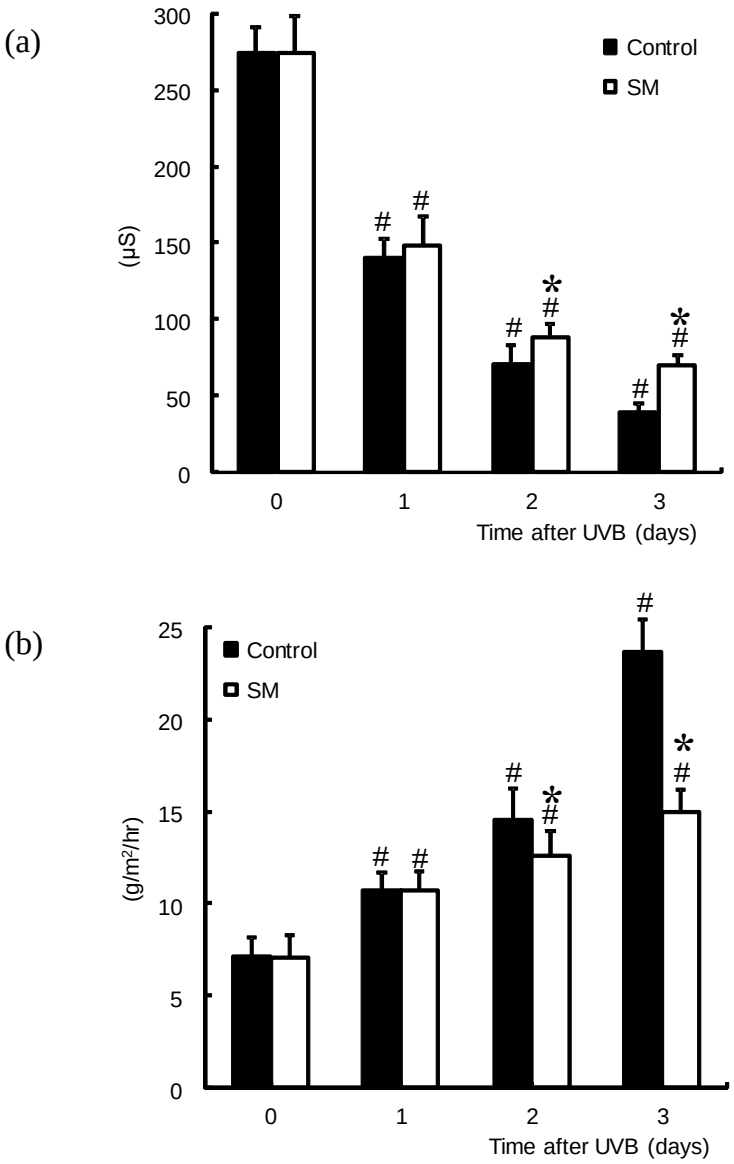

Fig. 17. Effect of SM on the SC water content (a) and TEWL (b) after UVB irradiation.

The values are shown as mean ± SD (n = 8/group). * $P < 0.05$ (vs. the control group), # $P < 0.05$ (vs. day 0).

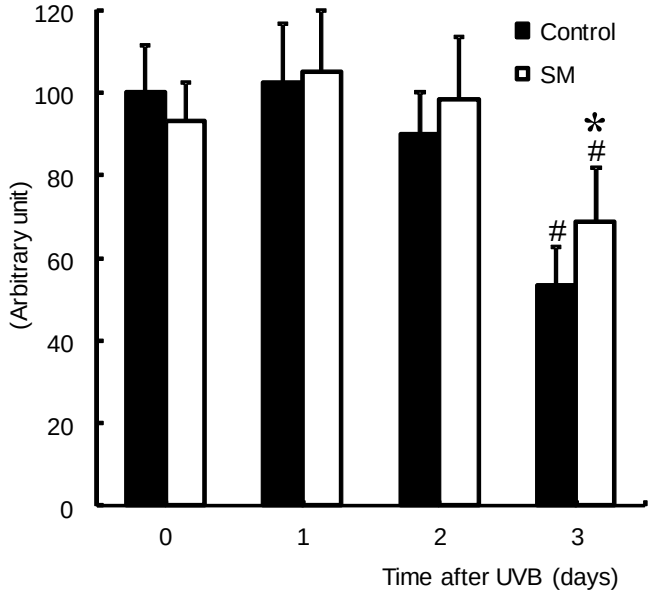

Fig. 18. Effect of SM on levels of covalently-bound ω-hydroxy ceramide in the epidermis induced by UVB irradiation.

Levels of ω-hydroxy tetratriacontenoic sphingoshine (d18:1-ω-hydroxy C34:1) are expressed as relative peak area per epidermal protein content.

The values are shown as mean ± SD (n = 8/group). * $P < 0.05$ (vs. the control group), # $P < 0.05$ (vs. day 0).

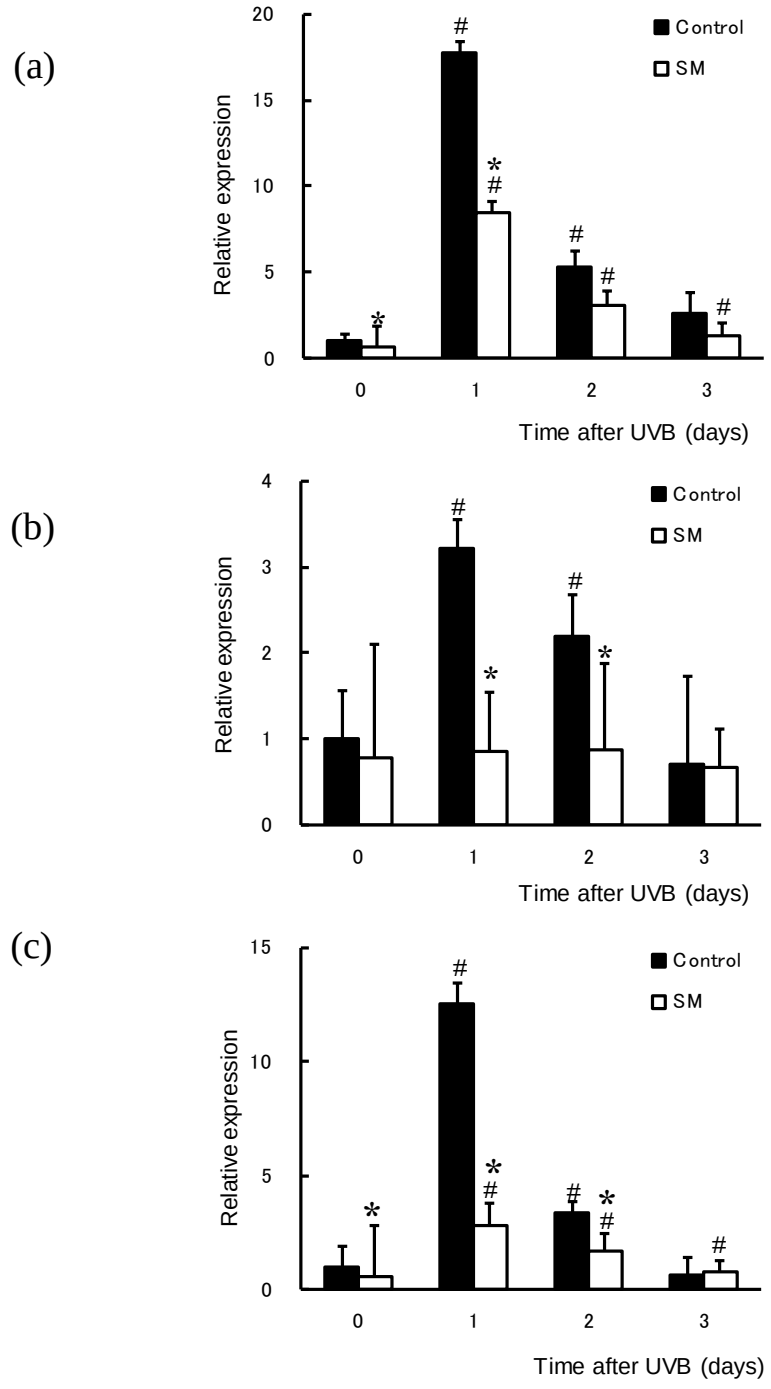

Fig. 19. Effect of SM on expression levels of TSLP (a), IL-1 beta (b) and IL-6 (c).

The mRNA levels are expressed as fold-change ± SD (SD of ΔCt) (n = 8/group). * $P < 0.05$ (vs. the control group), # $P < 0.05$ (vs. day 0).

(a)

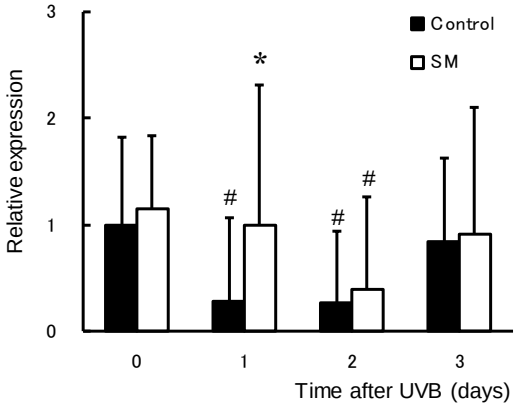

(b)

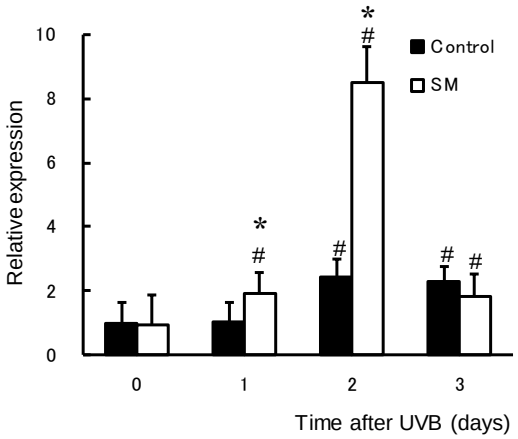

Fig. 20. Effect of SM on Loricrin (a) and TGase-3 (b) mRNA expression.

The mRNA levels are expressed as fold-change ± SD (SD of ΔCt) (n = 8/group). * P < 0.05 (vs. the control group). # P < 0.05 (vs. day 0).

4-4 Discussion

This study, demonstrated for the first time that SM administration could prevent photodamage, the disruption of skin barrier function, in hairless mice after a single dose of UVB irradiation. Furthermore, dietary SM suppressed a decrease in both the amount of protein-bound ω-hydroxy ceramides and loricrin mRNA levels. Together, these

results suggest that changes in epidermal structure markers, such as covalently-bound ω-hydroxy ceramide content and CE formations in mice fed milk derived-SM, might be associated with an improvement in skin barrier defects that are induced by UVB irradiation. One possible reason for this attenuation of skin barrier defects is that orally SM administration relieves skin inflammation, thereby promoting a decrease in the levels of covalently-bound ω-hydroxy ceramide. UVB irradiation is known to cause a decrease in ω-hydroxy ceramide levels in parallel with a significant increase in TEWL, however, the content of unbound ceramide increases (88). Therefore, covalently-bound ω-hydroxy ceramides in the epidermis are thought to play an important role in the formation of lamellar structures that participate in epidermal water retention. In previous section, ω-hydroxy tetratriacontenoic-sphingosine (d18:1-ω-hydroxy C34:1), the major molecular species of covalently-bound long-chain ω-hydroxy ceramides, were characterized from murine epidermises. The levels of this ceramide were significantly decreased after UVB exposure. UVB exposure accelerates release of pro-inflammatory mediators from various skin cells as well as the activation and subsequent infiltration of immune cells into the skin. The UVB-induced immune response usually begin with an abnormal release of inflammatory cytokines, including IL-1, IL-6, IL-8, and tumor necrosis factor-α (TNF-α) in keratinocytes (126-129). The results of this study are in agreement with these previous findings in that mRNA levels of the inflammation-associated genes TSLP, IL-1β and IL-6 were acutely up-regulated one day after a single dose of UVB irradiation prior to the manifestation of epidermal barrier dysfunction. Recent research showed that in human keratinocytes Th-2 cytokines such as IL-4 and IL-6 markedly decreased the production of esterified ω-hydroxy ceramides, which are precursors of covalently bound ω-hydroxy ceramides (130). Therefore, skin

inflammation induced by UVB exposure might suppress the formation of these ω-hydroxy ceramides in the epidermis. An interesting finding in this study was that dietary SM significantly suppressed an increase in the mRNA levels of inflammation-associated genes. One potential explanation of this result is that sphingolipids may themselves be a source of anti-inflammatory properties, as would be suggested by the potent protein kinase C inhibitory activity of sphingosine *in vitro* (131). Furthermore, treatment with sphingosine inhibited phorbol ester-induced skin inflammation via inactivation of protein kinase C in mice (132). Dietary glucosylceramide also suppressed the release of IL-1α in the skin of mice bred under dry skin conditions (133). Thus, dietary SM might attenuate skin inflammation and the decrease in covalently-bound ω-hydroxy ceramides, which together would result in improved skin barrier function. Another possible explanation of the changes in inflammation-related gene expression is that dietary SM may facilitate the formation of the CE. The epidermal CE is a complex protein-lipid composite that replaces the plasma membrane of terminally differentiated keratinocytes (134). This lamellar structure is crucial for the barrier function of skin and can prevent the loss of water and provide protection from environmental hazards. Loricrin is the major component of the CE in the epidermis, contributing as much as 70% of the CE mass (135-137), and provides a scaffold for the CE. Loricrin-deficient mice, furthermore, showed delayed formation of the skin barrier during embryonic development (138). Previous reports showed that a single exposure to UVB down-regulated loricrin, keratin 10, and filaggrin expression *in vitro* (139), which is in agreement with these *in vivo* results that also demonstrated that UVB irradiation decreased loricrin mRNA expression levels. Dietary SM suppressed these decreases in the mRNA level of loricrin following UVB exposure, while an

increase was observed in the mRNA levels of TGase-3. TGases are expressed mainly in the skin epidermis and play roles in CE formation during keratinocyte differentiation (85, 140). TGase-3 in particular promotes the cross-linking of loricrin and small proline-rich proteins to form small interchain oligomers that are then permanently cross-linked to the developing CE (141). Previous research reported that sphingosine, which is the major metabolite of sphingolipids, enhanced CE production and TGase-3 expression *in vitro* (142). Therefore, the sphingoid base might contribute to an increase in CE formation due to an activation of TGase-3. Consequently, I showed here that dietary SM stimulated mRNA levels of both loricrin and TGase-3, and enhanced the production of the CE in UVB damaged-skin, which in turn would improve skin barrier function. On the other hand, milk derived-phospholipid contains glycerophospholipids besides sphingolipids such as SM. Glycerophospholipids also have a potential to effect for the skin. Furthermore, previous reports revealed that oral supplementation with glucosylceramide improved skin barrier function (85, 142). Hydrolyzed SM form, such as ceramide, may represent potential active agent because SM and glucosylceramide are absorbed as the hydrolysate through intestines (143, 144). Further studies are needed to clarify contribution to the skin by type of sphingolipids.

Taken together, dietary SM prevented disruption of skin barrier function of hairless mouse induced by UVB irradiation. Furthermore, the administration of SM increased the strength of epidermal structures, due to an increase in both covalently-bound ceramide and CE formation. Further human studies needed because human has more complex SC and SC lipid composition with more comprehensive biosynthesis pathways. Dietary SM might thus modulate epidermal structures and prevent skin photodamage induced by UVB exposure.

CONCLUSION

Collagen hydrolysate and SM has a beneficial effect for preventing skin dysfunction such as the reduction of loss of epidermal barrier function and skin elasticity induced by UVB irradiation and chronological aging. The major findings presented in chapters 1 to 4 can be summarized as follows:

- Collagen hydrolysate administration suppressed epidermal barrier dysfunction and decrease in dermal skin elasticity in UVB irradiated skin.
- Collagen hydrolysate derived peptides may be associated with maintenance of dermal HA, which contributes to water capacity and elastic fiber in the skin, resulting anti-photoaging.
- Long-term oral intake of collagen hydrolysate improves intrinsic aging skin, that decreases in epidermal barrier function and skin elasticity.
- The altered gene expression at the early stages of collagen hydrolysate administration period may affect skin barrier function and mechanical properties by regulating genes related to production and maintenance of skin tissue.
- Long-term oral intake of SM containing phospholipids improves dry skin condition that decreases in epidermal barrier function.
- Dietary SM can modulate epidermal covalently-bound ceramides, key factors for skin barrier function maintenance, associated with formation of lamellar structures and suppress skin inflammation, resulting in improved skin barrier function.
- SM administration can prevent disruption of skin barrier function after UVB irradiation and modulate suppression of inflammation associated-gene expression, maintenance of covalently-bound ω-hydroxy ceramide content, and promotion of SC lamella structure associated-gene expression.

On the result of this study, it is emphasized that collagen hydrolysate facilitates generation of epidermis and maintenance of skin tissues, especially dermal HA and SM has critical roles in maintenance of these epidermal structure and effects for epidermal barrier function. However, since the results of this study are obtained from rats and mice, it is necessary to investigate the human dose.

In conclusion, continuous intake of dietary functional foods containing collagen hydrolysate and SM improved UVB induced- or chronological aged- skin damage and is favorable for homeostatic regulation of the skin. It is speculated that combination of use of ingestion of these components are more effective for attenuating intrinsic- or extrinsic aging induced skin damage. The author concluded that this thesis provided to create of “internal” -external beauty supplements based on dermatological evidence, and contributes to QOL improvement.

ACKNOWLEDGEMENTS

The author would like to express her sincere gratitude to Tatsuya Sugawara, Ph.D, Professor of division of Applied Biosciences, Graduate School of Agriculture, Kyoto University, for useful advice, helpful discussions and the kindest support and encouragements throughout this study.

The author greatly appreciates Yuji Nakai, Ph.D., Professor of Institute for Food Sciences, Hirosaki University, for many supports, valuable discussions, and useful suggestions during this study.

The author greatly appreciates Keiko Abe, Ph.D., Professor of Department of Applied Biological Chemistry, Graduate School of Agricultural and Life Sciences, The University of Tokyo, for helpful suggestion and valuable discussion.

The author greatly appreciates Tomoko Ishijima, Ph.D., Assistant professor of Department of Applied Biological Chemistry, Graduate School of Agricultural and Life Sciences, The University of Tokyo, for her experimental suggestion and valuable discussion.

The author would like to express my gratitude to the members of the laboratory of Meiji Co., Ltd, Hiroyuki Ito, Ph.D., Yukio Asami, Ph.D., Taketo Yamaji, Ph.D., Shuji Ikegami, Ph.D., Keiko Kawahata, Yukio Oshiba, Tomoyuki Fukasawa, Ph.D., Midori Natsume, Ph.D., Hiroki Ohara Ph.D., and Jinichiro Koga, Ph.D., Professor of Faculty of Science and Engineering, Teikyo University, and Hitoshi Matsumoto Ph.D., Professor of Faculty of Applied Life Sciences, Niigata University of Health and Welfare for their invaluable advices, helpful suggestions and sincere kindness.

The author would like to thank specially to Masashi Morifuji, Ph.D., Meiji Co., Ltd, for his invaluable advices, greatly encouragement and suggestion.

The author would like to thank the members of the laboratory of Meiji Co., Ltd, Kyoko Ito, Akiko Kusano, Satomi Ichikawa, Kumiko Fukuda, for their experimental work, technical assistance, supports and cheers.

Chisato Oba

REFERENCES

1. Moon SE, Youn JI and Kim JA The effect of ultraviolet-B exposure scheduling on the photodamage of hairless mouse skin. Photodermatol Photoimmunol Photomed. 2000; 16: 74-77.

2. Seidl E [ON THE EFFECTIVENESS OF DIFFERENT UV RAYS ON ERYTHEMA AND PIGMENTATION]. Strahlentherapie. 1963;121: 450-463.

3. Bissett DL, Hannon DP and Orr TV An animal model of solar-aged skin: histological, physical, and visible changes in UV-irradiated hairless mouse skin. Photochem Photobiol. 1987;46: 367-378.

4. Imokawa G Recent advances in characterizing biological mechanisms underlying UV-induced wrinkles: a pivotal role of fibrobrast-derived elastase. Arch Dermatol Res. 2008;300 Suppl 1: S7-20.

5. Abe T and Mayuzumi J The change and recovery of human skin barrier functions after ultraviolet light irradiation. Chem Pharm Bull (Tokyo). 1979;27: 458-462.

6. Cameron IL Cell proliferation and renewal in aging mice. J Gerontol. 1972;27: 162-172.

7. Neerken S, Lucassen GW, Bisschop MA, Lenderink E and Nuijs TA Characterization of age-related effects in human skin: A comparative study that applies confocal laser scanning microscopy and optical coherence tomography. J Biomed Opt. 2004;9: 274-281.

8. Haratake A, Uchida Y, Mimura K, Elias PM and Holleran WM Intrinsically aged epidermis displays diminished UVB-induced alterations in barrier function associated with decreased proliferation. J Invest Dermatol. 1997;108: 319-323.

9. Ghadially R, Brown BE, Sequeira-Martin SM, Feingold KR and Elias PM The aged

epidermal permeability barrier. Structural, functional, and lipid biochemical abnormalities in humans and a senescent murine model. J Clin Invest. 1995;95: 2281-2290.

10. Rogers J, Harding C, Mayo A, Banks J and Rawlings A Stratum corneum lipids: the effect of ageing and the seasons. Arch Dermatol Res. 1996;288: 765-770.

11. Hwang KA, Yi BR and Choi KC Molecular mechanisms and in vivo mouse models of skin aging associated with dermal matrix alterations. Lab Anim Res. 2011;27: 1-8.

12. Boelsma E, van de Vijver LP, Goldbohm RA, Klopping-Ketelaars IA, Hendriks HF and Roza L Human skin condition and its associations with nutrient concentrations in serum and diet. Am J Clin Nutr. 2003;77: 348-355.

13. Heinrich U, Neukam K, Tronnier H, Sies H and Stahl W Long-term ingestion of high flavanol cocoa provides photoprotection against UV-induced erythema and improves skin condition in women. J Nutr. 2006;136: 1565-1569.

14. Skovgaard GR, Jensen AS and Sigler ML Effect of a novel dietary supplement on skin aging in post-menopausal women. Eur J Clin Nutr. 2006;60: 1201-1206.

15. Schrieber R and Seybold U Gelatine production, the six steps to maximum safety. Dev Biol Stand. 1993;80: 195-198.

16. Ohara H, Matsumoto H, Ito K, Iwai K and Sato K Comparison of quantity and structures of Hyp-containing peptides in human blood after oral ingestion of gelatin hydrolysates from different sources. J Agric Food Chem. 2007;55: 1532-1535.

17. Ichikawa S, Morifuji M, Ohara H, Matsumoto H, Takeuchi Y and Sato K Hydroxyproline-containing dipeptides and tripeptides quantified at high concentration in human blood after oral administration of gelatin hydrolysate. Int J Food Sci Nutr. 2010;61: 52-60.

18. Postlethwaite AE, Seyer JM and Kang AH Chemotactic attraction of human fibroblasts to type I, II, and III collagens and collagen-derived peptides. Proc Natl Acad Sci U S A. 1978;75: 871-875.

19. Shigemura Y, Iwai K, Morimatsu F, Iwamoto T, Mori T, Oda C, Taira T, Park EY, Nakamura Y and Sato K Effect of Prolyl-hydroxyproline (Pro-Hyp), a food-derived collagen peptide in human blood, on growth of fibroblasts from mouse skin. J Agric Food Chem. 2009;57: 444-449.

20. Ohara H, Ichikawa S, Matsumoto H, Akiyama M, Fujimoto N, Kobayashi T and Tajima S Collagen-derived dipeptide, proline-hydroxyproline, stimulates cell proliferation and hyaluronic acid synthesis in cultured human dermal fibroblasts. J Dermatol. 2010;37: 330-338.

21. Zague V, de Freitas V, da Costa Rosa M, de Castro GA, Jaeger RG and Machado-Santelli GM Collagen hydrolysate intake increases skin collagen expression and suppresses matrix metalloproteinase 2 activity. J Med Food. 2011;14: 618-624.

22. Tanaka M, Koyama Y and Nomura Y Effects of collagen peptide ingestion on UV-B-induced skin damage. Biosci Biotechnol Biochem. 2009;73: 930-932.

23. Hirotsune M, Haratake A, Komiya A, Sugita J, Tachihara T, Komai T, Hizume K, Ozeki K and Ikemoto T Effect of ingested concentrate and components of sake on epidermal permeability barrier disruption by UVB irradiation. J Agric Food Chem. 2005;53: 948-952.

24. Takagi Y, Nakagawa H, Yaginuma T, Takema Y and Imokawa G An accumulation of glucosylceramide in the stratum corneum due to attenuated activity of beta-glucocerebrosidase is associated with the early phase of UVB-induced alteration in cutaneous barrier function. Arch Dermatol Res. 2005;297: 18-25.

25. Tsukahara K, Nakagawa H, Moriwaki S, Kakuo S, Ohuchi A, Takema Y and Imokawa G Ovariectomy is sufficient to accelerate spontaneous skin ageing and to stimulate ultraviolet irradiation-induced photoageing of murine skin. Br J Dermatol. 2004;151: 984-994.

26. Cho HS, Lee MH, Lee JW, No KO, Park SK, Lee HS, Kang S, Cho WG, Park HJ, Oh KW and Hong JT Anti-wrinkling effects of the mixture of vitamin C, vitamin E, pycnogenol and evening primrose oil, and molecular mechanisms on hairless mouse skin caused by chronic ultraviolet B irradiation. Photodermatol Photoimmunol Photomed. 2007;23: 155-162.

27. Reeves PG, Nielsen FH and Fahey GC, Jr. AIN-93 purified diets for laboratory rodents: final report of the American Institute of Nutrition ad hoc writing committee on the reformulation of the AIN-76A rodent diet. J Nutr. 1993;123: 1939-1951.

28. Margelin D, Medaisko C, Lombard D, Picard J and Fourtanier A Hyaluronic acid and dermatan sulfate are selectively stimulated by retinoic acid in irradiated and nonirradiated hairless mouse skin. J Invest Dermatol. 1996;106: 505-509.

29. Tobiishi M, Sayo T, Yoshida H, Kusaka A, Kawabata K, Sugiyama Y, Ishikawa O and Inoue S Changes in epidermal hyaluronan metabolism following UVB irradiation. J Dermatol Sci. 2011;64: 31-38.

30. Haratake A, Uchida Y, Schmuth M, Tanno O, Yasuda R, Epstein JH, Elias PM and Holleran WM UVB-induced alterations in permeability barrier function: roles for epidermal hyperproliferation and thymocyte-mediated response. J Invest Dermatol. 1997;108: 769-775.

31. Inomata S, Matsunaga Y, Amano S, Takada K, Kobayashi K, Tsunenaga M, Nishiyama T, Kohno Y and Fukuda M Possible involvement of gelatinases in basement

membrane damage and wrinkle formation in chronically ultraviolet B-exposed hairless mouse. J Invest Dermatol. 2003;120: 128-134.

32. Laurent TC and Fraser JR Hyaluronan. FASEB J. 1992;6: 2397-2404.

33. Dai G, Freudenberger T, Zipper P, Melchior A, Grether-Beck S, Rabausch B, de Groot J, Twarock S, Hanenberg H, Homey B, Krutmann J, Reifenberger J and Fischer JW Chronic ultraviolet B irradiation causes loss of hyaluronic acid from mouse dermis because of down-regulation of hyaluronic acid synthases. Am J Pathol. 2007;171: 1451-1461.

34. Gu H, Huang L, Wong YP and Burd A HA modulation of epidermal morphogenesis in an organotypic keratinocyte-fibroblast co-culture model. Exp Dermatol. 2010;19: e336-339.

35. Okawa T, Yamaguchi Y, Takada S, Sakai Y, Numata N, Nakamura F, Nagashima Y, Ikezawa Z and Aihara M Oral administration of collagen tripeptide improves dryness and pruritus in the acetone-induced dry skin model. J Dermatol Sci. 2012;66: 136-143.

36. Kawaguchi T, Nanbu PN and Kurokawa M Distribution of prolylhydroxyproline and its metabolites after oral administration in rats. Biol Pharm Bull. 2012;35: 422-427.

37. Liang J, Pei X, Zhang Z, Wang N, Wang J and Li Y The protective effects of long-term oral administration of marine collagen hydrolysate from chum salmon on collagen matrix homeostasis in the chronological aged skin of Sprague-Dawley male rats. J Food Sci. 2010;75: H230-238.

38. Proksch E, Schunck M, Zague V, Segger D, Degwert J and Oesser S Oral intake of specific bioactive collagen peptides reduces skin wrinkles and increases dermal matrix synthesis. Skin Pharmacol Physiol. 2014;27: 113-119.

39. Yoon HS, Cho HH, Cho S, Lee SR, Shin MH and Chung JH Supplementating with

dietary astaxanthin combined with collagen hydrolysate improves facial elasticity and decreases matrix metalloproteinase-1 and -12 expression: a comparative study with placebo. J Med Food. 2014;17: 810-816.

40. Fukasawa T, Kamei A, Watanabe Y, Koga J and Abe K Short-chain fructooligosaccharide regulates hepatic peroxisome proliferator-activated receptor alpha and farnesoid X receptor target gene expression in rats. J Agric Food Chem. 2010;58: 7007-7012.

41. Kanda A, Ishijima T, Shinozaki F, Nakayama K, Fukasawa T, Nakai Y, Abe K, Kawahata K and Ikegami S Post-exercise impact of ingested whey protein hydrolysate on gene expression profiles in rat skeletal muscle: activation of extracellular signal-regulated kinase 1/2 and hypoxia-inducible factor-1alpha. Br J Nutr. 2014;111: 2067-2078.

42. Schroeder A, Mueller O, Stocker S, Salowsky R, Leiber M, Gassmann M, Lightfoot S, Menzel W, Granzow M and Ragg T The RIN: an RNA integrity number for assigning integrity values to RNA measurements. BMC Mol Biol. 2006;7: 3.

43. Suyama T, Okada S, Ishijima T, Iida K, Abe K and Nakai Y High phosphorus diet-induced changes in NaPi-IIb phosphate transporter expression in the rat kidney: DNA microarray analysis. PLoS One. 2012;7: e29483.

44. Chen Z, McGee M, Liu Q and Scheuermann RH A distribution free summarization method for Affymetrix GeneChip arrays. Bioinformatics. 2007;23: 321-327.

45. Team RDC (2006) A Language and Environment for Statistical Computing. .

46. Gentleman RC, Carey VJ, Bates DM, Bolstad B, Dettling M, Dudoit S, Ellis B, Gautier L, Ge Y, Gentry J, Hornik K, Hothorn T, Huber W, Iacus S, Irizarry R, Leisch F, Li C, Maechler M, Rossini AJ, Sawitzki G, Smith C, Smyth G, Tierney L, Yang JY and

Zhang J Bioconductor: open software development for computational biology and bioinformatics. Genome Biol. 2004;5: R80.

47. Suzuki R and Shimodaira H Pvclust: an R package for assessing the uncertainty in hierarchical clustering. Bioinformatics. 2006;22: 1540-1542.

48. Breitling R, Armengaud P, Amtmann A and Herzyk P Rank products: a simple, yet powerful, new method to detect differentially regulated genes in replicated microarray experiments. FEBS Lett. 2004;573: 83-92.

49. Benjamini Y and Hochberg Y Controlling the False Discovery Rate: A Practical and Powerful Approach to Multiple Testing. J R Stat Soc Ser B. 1995;57: 289-300.

50. Kamei A, Watanabe Y, Ishijima T, Uehara M, Arai S, Kato H, Nakai Y and Abe K Dietary iron-deficient anemia induces a variety of metabolic changes and even apoptosis in rat liver: a DNA microarray study. Physiol Genomics. 2010;42: 149-156.

51. Huang da W, Sherman BT and Lempicki RA Systematic and integrative analysis of large gene lists using DAVID bioinformatics resources. Nat Protoc. 2009;4: 44-57.

52. Binns D, Dimmer E, Huntley R, Barrell D, O'Donovan C and Apweiler R QuickGO: a web-based tool for Gene Ontology searching. Bioinformatics. 2009;25: 3045-3046.

53. Biosystems A (1997) User Bulletin #2 Applied Biosystems.

54. Schmittgen TD and Livak KJ Analyzing real-time PCR data by the comparative C(T) method. Nat Protoc. 2008;3: 1101-1108.

55. Marshall D, Hardman MJ and Byrne C SPRR1 gene induction and barrier formation occur as coordinated moving fronts in terminally differentiating epithelia. J Invest Dermatol. 2000;114: 967-975.

56. Cerimele D, Celleno L and Serri F Physiological changes in ageing skin. Br J Dermatol. 1990;122 Suppl 35: 13-20.

57. Shirakata Y, Komurasaki T, Toyoda H, Hanakawa Y, Yamasaki K, Tokumaru S, Sayama K and Hashimoto K Epiregulin, a novel member of the epidermal growth factor family, is an autocrine growth factor in normal human keratinocytes. J Biol Chem. 2000;275: 5748-5753.

58. Huber M, Siegenthaler G, Mirancea N, Marenholz I, Nizetic D, Breitkreutz D, Mischke D and Hohl D Isolation and characterization of human repetin, a member of the fused gene family of the epidermal differentiation complex. J Invest Dermatol. 2005;124: 998-1007.

59. Eckert RL, Yaffe MB, Crish JF, Murthy S, Rorke EA and Welter JF Involucrin--structure and role in envelope assembly. J Invest Dermatol. 1993;100: 613-617.

60. Steinert PM, Candi E, Kartasova T and Marekov L Small proline-rich proteins are cross-bridging proteins in the cornified cell envelopes of stratified squamous epithelia. J Struct Biol. 1998;122: 76-85.

61. Scott DK, Lord R, Muller HK, Malley RC and Woods GM Proteomics identifies enhanced expression of stefin A in neonatal murine skin compared with adults: functional implications. Br J Dermatol. 2007;156: 1156-1162.

62. Swartzendruber DC, Wertz PW, Madison KC and Downing DT Evidence that the corneocyte has a chemically bound lipid envelope. J Invest Dermatol. 1987;88: 709-713.

63. Presland RB and Dale BA Epithelial structural proteins of the skin and oral cavity: function in health and disease. Crit Rev Oral Biol Med. 2000;11: 383-408.

64. Hanakawa Y, Amagai M, Shirakata Y, Yahata Y, Tokumaru S, Yamasaki K, Tohyama M, Sayama K and Hashimoto K Differential effects of desmoglein 1 and

desmoglein 3 on desmosome formation. J Invest Dermatol. 2002;119: 1231-1236.

65. Boury-Jamot M, Daraspe J, Bonte F, Perrier E, Schnebert S, Dumas M and Verbavatz JM Skin aquaporins: function in hydration, wound healing, and skin epidermis homeostasis. Handb Exp Pharmacol. 2009: 205-217.

66. Hara-Chikuma M and Verkman AS Roles of aquaporin-3 in the epidermis. J Invest Dermatol. 2008;128: 2145-2151.

67. Li J, Tang H, Hu X, Chen M and Xie H Aquaporin-3 gene and protein expression in sun-protected human skin decreases with skin ageing. Australas J Dermatol. 2010;51: 106-112.

68. Hara M, Ma T and Verkman AS Selectively reduced glycerol in skin of aquaporin-3-deficient mice may account for impaired skin hydration, elasticity, and barrier recovery. J Biol Chem. 2002;277: 46616-46621.

69. Kim SH, Turnbull J and Guimond S Extracellular matrix and cell signalling: the dynamic cooperation of integrin, proteoglycan and growth factor receptor. J Endocrinol. 2011;209: 139-151.

70. Nagase H and Woessner JF, Jr. Matrix metalloproteinases. J Biol Chem. 1999;274: 21491-21494.

71. Vlodavsky I, Ilan N, Naggi A and Casu B Heparanase: structure, biological functions, and inhibition by heparin-derived mimetics of heparan sulfate. Curr Pharm Des. 2007;13: 2057-2073.

72. Woessner JF, Jr. Matrix metalloproteinases and their inhibitors in connective tissue remodeling. FASEB J. 1991;5: 2145-2154.

73. Mays PK, McAnulty RJ, Campa JS and Laurent GJ Age-related changes in collagen synthesis and degradation in rat tissues. Importance of degradation of newly synthesized

collagen in regulating collagen production. Biochem J. 1991;276 (Pt 2): 307-313.

74. Shimizu J, Asami N, Kataoka A, Sugihara F, Inoue N, Kimira Y, Wada M and Mano H Oral collagen-derived dipeptides, prolyl-hydroxyproline and hydroxyprolyl-glycine, ameliorate skin barrier dysfunction and alter gene expression profiles in the skin. Biochem Biophys Res Commun. 2015;456: 626-630.

75. Postlethwaite AE, Seyer JM and Kang AH Chemotactic attraction of human fibroblasts to type I, II, and III collagens and collagen-derived peptides. Proc Natl Acad Sci U S A. 1978;75: 871-875.

76. Le Vu P, Takatori R, Iwamoto T, Akagi Y, Satsu H, Totsuka M, Chida K, Sato K and Shimizu M Effects of Food-Derived Collagen Peptides on the Expression of Keratin and Keratin-Associated Protein Genes in the Mouse Skin. Skin Pharmacol Physiol. 2015;28: 227-235.

77. Haruta Y, Kato K and Yoshioka T Dietary phospholipid concentrate from bovine milk improves epidermal function in hairless mice. Biosci Biotechnol Biochem. 2008;72: 2151-2157.

78. Vesper H, Schmelz EM, Nikolova-Karakashian MN, Dillehay DL, Lynch DV and Merrill AH, Jr. Sphingolipids in food and the emerging importance of sphingolipids to nutrition. J Nutr. 1999;129: 1239-1250.

79. Zeisel SH, Char D and Sheard NF Choline, phosphatidylcholine and sphingomyelin in human and bovine milk and infant formulas. J Nutr. 1986;116: 50-58.

80. Zeisel SH, Mar MH, Howe JC and Holden JM Concentrations of choline-containing compounds and betaine in common foods. J Nutr. 2003;133: 1302-1307.

81. Watanabe S, Takahashi T, Tanaka L, Haruta Y, Shiota M, Hosokawa M and Miyashita K The effect of milk polar lipids separated from butter serum on the lipid

levels in the liver and the plasma of obese-model mouse (KK-Ay). J Funct Foods. 2011;3: 313-320.

82. Schmelz EM, Dillehay DL, Webb SK, Reiter A, Adams J and Merrill AH, Jr. Sphingomyelin consumption suppresses aberrant colonic crypt foci and increases the proportion of adenomas versus adenocarcinomas in CF1 mice treated with 1,2-dimethylhydrazine: implications for dietary sphingolipids and colon carcinogenesis. Cancer Res. 1996;56: 4936-4941.

83. Schmelz EM, Bushnev AS, Dillehay DL, Liotta DC and Merrill AH, Jr. Suppression of aberrant colonic crypt foci by synthetic sphingomyelins with saturated or unsaturated sphingoid base backbones. Nutr Cancer. 1997;28: 81-85.

84. Haruta-Ono Y, Setoguchi S, Ueno HM, Higurashi S, Ueda N, Kato K, Saito T, Matsunaga K and Takata J Orally administered sphingomyelin in bovine milk is incorporated into skin sphingolipids and is involved in the water-holding capacity of hairless mice. J Dermatol Sci. 2012;68: 56-62.

85. Ideta R, Sakuta T, Nakano Y and Uchiyama T Orally administered glucosylceramide improves the skin barrier function by upregulating genes associated with the tight junction and cornified envelope formation. Biosci Biotechnol Biochem. 2011;75: 1516-1523.

86. Kim H, Lee J and Cho Y Dietary sericin enhances epidermal levels of glucosylceramides and ceramides with up-regulating protein expressions of glucosylceramide synthase, beta-glucocerebrosidase and acidic sphingomyelinase in NC/Nga mice. Nutr Res. 2012;32: 956-964.

87. Kim J and Cho Y Gromwell (Lithospermum erythrorhizon) supplementation enhances epidermal levels of ceramides, glucosylceramides, beta-glucocerebrosidase,

and acidic sphingomyelinase in NC/Nga mice. J Med Food. 2013;16: 927-933.

88. Takagi Y, Nakagawa H, Kondo H, Takema Y and Imokawa G Decreased levels of covalently bound ceramide are associated with ultraviolet B-induced perturbation of the skin barrier. J Invest Dermatol. 2004;123: 1102-1109.

89. Meguro S, Arai Y, Masukawa Y, Uie K and Tokimitsu I Relationship between covalently bound ceramides and transepidermal water loss (TEWL). Arch Dermatol Res. 2000;292: 463-468.

90. Behne M, Uchida Y, Seki T, de Montellano PO, Elias PM and Holleran WM Omega-hydroxyceramides are required for corneocyte lipid envelope (CLE) formation and normal epidermal permeability barrier function. J Invest Dermatol. 2000;114: 185-192.

91. Leung DY, Boguniewicz M, Howell MD, Nomura I and Hamid QA New insights into atopic dermatitis. J Clin Invest. 2004;113: 651-657.

92. Kakinuma T, Nakamura K, Wakugawa M, Mitsui H, Tada Y, Saeki H, Torii H, Asahina A, Onai N, Matsushima K and Tamaki K Thymus and activation-regulated chemokine in atopic dermatitis: Serum thymus and activation-regulated chemokine level is closely related with disease activity. J Allergy Clin Immunol. 2001;107: 535-541.

93. Alysandratos KD, Angelidou A, Vasiadi M, Zhang B, Kalogeromitros D, Katsarou-Katsari A and Theoharides TC Increased affected skin gene expression and serum levels of thymic stromal lymphopoietin in atopic dermatitis. Ann Allergy Asthma Immunol. 2010;105: 403-404.

94. Tamagawa-Mineoka R, Katoh N, Ueda E, Masuda K and Kishimoto S Platelet-derived microparticles and soluble P-selectin as platelet activation markers in

patients with atopic dermatitis. Clin Immunol. 2009;131: 495-500.

95. Duan J, Sugawara T, Hirose M, Aida K, Sakai S, Fujii A and Hirata T Dietary sphingolipids improve skin barrier functions via the upregulation of ceramide synthases in the epidermis. Exp Dermatol. 2012;21: 448-452.

96. Fujii M, Akita K, Mizutani N, Nabe T and Kohno S Development of numerous nerve fibers in the epidermis of hairless mice with atopic dermatitis-like pruritic skin inflammation. J Pharmacol Sci. 2007;104: 243-251.

97. Fujii M, Nakashima H, Tomozawa J, Shimazaki Y, Ohyanagi C, Kawaguchi N, Ohya S, Kohno S and Nabe T Deficiency of n-6 polyunsaturated fatty acids is mainly responsible for atopic dermatitis-like pruritic skin inflammation in special diet-fed hairless mice. Exp Dermatol. 2013;22: 272-277.

98. Fujii M, Tomozawa J, Mizutani N, Nabe T, Danno K and Kohno S Atopic dermatitis-like pruritic skin inflammation caused by feeding a special diet to HR-1 hairless mice. Exp Dermatol. 2005;14: 460-468.

99. Macheleidt O, Kaiser HW and Sandhoff K Deficiency of epidermal protein-bound omega-hydroxyceramides in atopic dermatitis. J Invest Dermatol. 2002;119: 166-173.

100. Schmittgen TD and Livak KJ Analyzing real-time PCR data by the comparative C(T) method. Nat Protoc. 2008;3: 1101-1108.

101. Shimada E, Aida K, Sugawara T and Hirata T Inhibitory effect of topical maize glucosylceramide on skin photoaging in UVA-irradiated hairless mice. J Oleo Sci. 2011;60: 321-325.

102. Masukawa Y, Narita H, Sato H, Naoe A, Kondo N, Sugai Y, Oba T, Homma R, Ishikawa J, Takagi Y and Kitahara T Comprehensive quantification of ceramide species in human stratum corneum. J Lipid Res. 2009;50: 1708-1719.

103. Ishikawa J, Narita H, Kondo N, Hotta M, Takagi Y, Masukawa Y, Kitahara T, Takema Y, Koyano S, Yamazaki S and Hatamochi A Changes in the ceramide profile of atopic dermatitis patients. J Invest Dermatol. 2010;130: 2511-2514.

104. Bouwstra JA, Gooris GS, Dubbelaar FE and Ponec M Phase behavior of stratum corneum lipid mixtures based on human ceramides: the role of natural and synthetic ceramide 1. J Invest Dermatol. 2002;118: 606-617.

105. Tsuji K, Mitsutake S, Ishikawa J, Takagi Y, Akiyama M, Shimizu H, Tomiyama T and Igarashi Y Dietary glucosylceramide improves skin barrier function in hairless mice. J Dermatol Sci. 2006;44: 101-107.

106. Sugawara T, Tsuduki T, Yano S, Hirose M, Duan J, Aida K, Ikeda I and Hirata T Intestinal absorption of dietary maize glucosylceramide in lymphatic duct cannulated rats. J Lipid Res. 2010;51: 1761-1769.

107. Nilsson A Metabolism of cerebroside in the intestinal tract of the rat. Biochim Biophys Acta. 1969;187: 113-121.

108. Nilsson A Metabolism of sphingomyelin in the intestinal tract of the rat. Biochim Biophys Acta. 1968;164: 575-584.

109. Schmelz EM, Crall KJ, Larocque R, Dillehay DL and Merrill AH, Jr. Uptake and metabolism of sphingolipids in isolated intestinal loops of mice. J Nutr. 1994;124: 702-712.

110. Hasegawa T, Shimada H, Uchiyama T, Ueda O, Nakashima M and Matsuoka Y Dietary glucosylceramide enhances cornified envelope formation via transglutaminase expression and involucrin production. Lipids. 2011;46: 529-535.

111. Byrdwell WC and Perry RH Liquid chromatography with dual parallel mass spectrometry and 31P nuclear magnetic resonance spectroscopy for analysis of

sphingomyelin and dihydrosphingomyelin. II. Bovine milk sphingolipids. J Chromatogr A. 2007;1146: 164-185.

112. Liu YJ Thymic stromal lymphopoietin: master switch for allergic inflammation. J Exp Med. 2006;203: 269-273.

113. Liu YJ, Soumelis V, Watanabe N, Ito T, Wang YH, Malefyt Rde W, Omori M, Zhou B and Ziegler SF TSLP: an epithelial cell cytokine that regulates T cell differentiation by conditioning dendritic cell maturation. Annu Rev Immunol. 2007;25: 193-219.

114. Soumelis V, Reche PA, Kanzler H, Yuan W, Edward G, Homey B, Gilliet M, Ho S, Antonenko S, Lauerma A, Smith K, Gorman D, Zurawski S, Abrams J, Menon S, McClanahan T, de Waal-Malefyt Rd R, Bazan F, Kastelein RA and Liu YJ Human epithelial cells trigger dendritic cell mediated allergic inflammation by producing TSLP. Nat Immunol. 2002;3: 673-680.

115. Hannun YA and Bell RM Regulation of protein kinase C by sphingosine and lysosphingolipids. Clin Chim Acta. 1989;185: 333-345.

116. Gupta AK, Fisher GJ, Elder JT, Nickoloff BJ and Voorhees JJ Sphingosine inhibits phorbol ester-induced inflammation, ornithine decarboxylase activity, and activation of protein kinase C in mouse skin. J Invest Dermatol. 1988;91: 486-491.

117. Duan J, Sugawara T, Sakai S, Aida K and Hirata T Oral glucosylceramide reduces 2,4-dinitrofluorobenzene induced inflammatory response in mice by reducing TNF-alpha levels and leukocyte infiltration. Lipids. 2011;46: 505-512.

118. Jin H, He R, Oyoshi M and Geha RS Animal models of atopic dermatitis. J Invest Dermatol. 2009;129: 31-40.

119. Tanaka A, Amagai Y, Oida K and Matsuda H Recent findings in mouse models for

human atopic dermatitis. Exp Anim. 2012;61: 77-84.

120. Holleran WM, Uchida Y, Halkier-Sorensen L, Haratake A, Hara M, Epstein JH and Elias PM Structural and biochemical basis for the UVB-induced alterations in epidermal barrier function. Photodermatol Photoimmunol Photomed. 1997;13: 117-128.

121. Brod J Characterization and physiological role of epidermal lipids. Int J Dermatol. 1991;30: 84-90.

122. Meguro S, Arai Y, Masukawa Y, Uie K and Tokimitsu I Relationship between covalently bound ceramides and transepidermal water loss (TEWL). Arch Dermatol Res. 2000;292: 463-468.

123. Hitomi K Transglutaminases in skin epidermis. Eur J Dermatol. 2005;15: 313-319.

124. Chomczynski P and Sacchi N Single-step method of RNA isolation by acid guanidinium thiocyanate-phenol-chloroform extraction. Anal Biochem. 1987;162: 156-159.

125. Schmittgen TD and Livak KJ Analyzing real-time PCR data by the comparative C(T) method. Nat Protoc. 2008;3: 1101-1108.

126. Kupper TS, Chua AO, Flood P, McGuire J and Gubler U Interleukin 1 gene expression in cultured human keratinocytes is augmented by ultraviolet irradiation. J Clin Invest. 1987;80: 430-436.

127. Kondo S, Kono T, Sauder DN and McKenzie RC IL-8 gene expression and production in human keratinocytes and their modulation by UVB. J Invest Dermatol. 1993;101: 690-694.

128. Kulms D, Poppelmann B and Schwarz T Ultraviolet radiation-induced interleukin 6 release in HeLa cells is mediated via membrane events in a DNA damage-independent way. J Biol Chem. 2000;275: 15060-15066.

129. Bashir MM, Sharma MR and Werth VP UVB and proinflammatory cytokines synergistically activate TNF-alpha production in keratinocytes through enhanced gene transcription. J Invest Dermatol. 2009;129: 994-1001.

130. Sawada E, Yoshida N, Sugiura A and Imokawa G Th1 cytokines accentuate but Th2 cytokines attenuate ceramide production in the stratum corneum of human epidermal equivalents: an implication for the disrupted barrier mechanism in atopic dermatitis. J Dermatol Sci. 2012;68: 25-35.

131. Hannun YA and Bell RM Regulation of protein kinase C by sphingosine and lysosphingolipids. Clin Chim Acta. 1989;185: 333-345.

132. Gupta AK, Fisher GJ, Elder JT, Nickoloff BJ and Voorhees JJ Sphingosine inhibits phorbol ester-induced inflammation, ornithine decarboxylase activity, and activation of protein kinase C in mouse skin. J Invest Dermatol. 1988;91: 486-491.

133. Uchiyama T, Nakano Y, Ueda O, Mori H, Nakashima M, Noda A, Ishizaki C and Mizoguchi M Oral Intake of Glucosylceramide Improves Relatively Higher Level of Transepidermal Water Loss in Mice and Healthy Human Subjects. J Health Sci. 2008;54: 559-566.

134. Roop D Defects in the barrier. Science. 1995;267: 474-475.

135. Hohl D, Mehrel T, Lichti U, Turner ML, Roop DR and Steinert PM Characterization of human loricrin. Structure and function of a new class of epidermal cell envelope proteins. J Biol Chem. 1991;266: 6626-6636.

136. Steven AC and Steinert PM Protein composition of cornified cell envelopes of epidermal keratinocytes. J Cell Sci. 1994;107 (Pt 2): 693-700.

137. Kalinin A, Marekov LN and Steinert PM Assembly of the epidermal cornified cell envelope. J Cell Sci. 2001;114: 3069-3070.

138. Koch PJ, de Viragh PA, Scharer E, Bundman D, Longley MA, Bickenbach J, Kawachi Y, Suga Y, Zhou Z, Huber M, Hohl D, Kartasova T, Jarnik M, Steven AC and Roop DR Lessons from loricrin-deficient mice: compensatory mechanisms maintaining skin barrier function in the absence of a major cornified envelope protein. J Cell Biol. 2000;151: 389-400.

139. Bernerd F and Asselineau D Successive alteration and recovery of epidermal differentiation and morphogenesis after specific UVB-damages in skin reconstructed in vitro. Dev Biol. 1997;183: 123-138.

140. Eckert RL, Sturniolo MT, Broome AM, Ruse M and Rorke EA Transglutaminase function in epidermis. J Invest Dermatol. 2005;124: 481-492.

141. Candi E, Tarcsa E, Idler WW, Kartasova T, Marekov LN and Steinert PM Transglutaminase cross-linking properties of the small proline-rich 1 family of cornified cell envelope proteins. Integration with loricrin. J Biol Chem. 1999;274: 7226-7237.

142. Hasegawa T, Shimada H, Uchiyama T, Ueda O, Nakashima M and Matsuoka Y Dietary glucosylceramide enhances cornified envelope formation via transglutaminase expression and involucrin production. Lipids. 2011;46: 529-535.

143. Schmelz EM, Crall KJ, Larocque R, Dillehay DL and Merrill AH, Jr. Uptake and metabolism of sphingolipids in isolated intestinal loops of mice. J Nutr. 1994;124: 702-712.

144. Sugawara T, Kinoshita M, Ohnishi M, Nagata J and Saito M Digestion of maize sphingolipids in rats and uptake of sphingadienine by Caco-2 cells. J Nutr. 2003;133: 2777-2782.

LIST OF PUBLICATIONS

1. Oba C, Ohara H, Morifuji M, Ito K, Ichikawa S, Kawahata K and Koga J Collagen hydrolysate intake improves the loss of epidermal barrier function and skin elasticity induced by UVB irradiation in hairless mice. Photodermatol Photoimmunol Photomed. 2013;29: 204-211.

2. Oba C, Ito K, Ichikawa S, Morifuji M, Nakai Y, Ishijima T, Abe K and Kawahata K Effect of orally administered collagen hydrolysate on gene expression profiles in mouse skin: a DNA microarray analysis. Physiol Genomics. 2015;47: 355-363.

3. Morifuji M, Oba C, Ichikawa S, Ito K, Kawahata K, Asami Y, Ikegami S, Itoh H and Sugawara T A novel mechanism for improvement of dry skin by dietary milk phospholipids: Effect on epidermal covalently bound ceramides and skin inflammation in hairless mice. J Dermatol Sci. 2015;78: 224-231.

4. Oba C, Morifuji M, Ichikawa S, Ito K, Kawahata K, Yamaji T, Asami Y, Itou H and Sugawara T Dietary Milk Sphingomyelin Prevents Disruption of Skin Barrier Function in Hairless Mice after UV-B Irradiation. PLoS One. 2015;10: e0136377.